PEG-Hydrogel Coated Silica Aerogels / A Novel Drug Delivery System

by

Seda Giray

A Thesis Submitted to the
Graduate School of Engineering
in Partial Fulfillment of the Requirements for
the Degree of

Master of Science
in
Chemical and Biological Engineering

Koç University
September 2010

Koç University

Graduate School of Sciences and Engineering

This is to certify that I have examined this copy of a master's thesis by

Seda Giray

and have found that it is complete and satisfactory in all respects,
and that any and all revisions required by the final
examining committee have been made.

Committee Members:

Prof. Dr. Can Erkey

Assist. Prof. Dr. Seda Kızılel

Prof. Dr. Şevket Ruacan

Date: 20.09.2010

Dedicted to my sister, **Başak**
and to my cat, **Poça**

ABSTRACT

A novel composite of silica aerogel and poly (ethylene glycol) PEG hydrogel was synthesized and its potential as a drug delivery system were investigated. The composite was synthesized by encapsulation of hydrophobic aerogels within PEG hydrogel via photoinitiated polymerization. Disks of aerogels were synthesized by the two step sol-gel method using tetraethylortosilicate (TEOS) as the silica precursor. After the gels were aged in ethanol, the alcogels were then contacted with a solution of eosin-Y, a photoinitiator, dissolved in ethanol. The adsorption of eosin-Y onto the surface of alcogel led to a reddish transparent composite of silica aerogel with eosin-Y. The surface of eosin functionalized silica aerogels was then rendered hydrophobic using hexamethyldisilazane (HMDS) as the surface modification agent, and supercritical carbon dioxide ($ScCO_2$) as solvent. Hydrophobicity of aerogel was tuned by changing HMDS amount dissolved in $ScCO_2$ phase which changes the contact angle between 0-128^o. Hydrophobic or hydrophilic aerogels were then dipped into a PEG diacrylate prepolymer solution, and photopolymerization was carried out using visible light (514 nm). BET surface area and pore size distribution measurements show that both hydrogel encapsulation and eosin-Y loading did not affect the pore structure of the aerogel.

The potential of this novel composite as a drug delivery system was tested by Ketoprofen as a model drug. The results demonstrate that both drug loading capacity and drug release profiles could be tuned by changing hydrophobicity of aerogels, and that drug loading capacity increases with decreased aerogel hydrophobicity while slower release rates are achieved with increased hydrophobicity from eosin functionalized aerogels. The effect of PEG concentration (0, 15 %, and 30 % w/w) in the prepolymer solution of the hydrogel coating on drug release rate from hydrophilic aerogel was also investigated. It was seen that as the PEG concentration increased, the drug release was retarded. The experimental results showed that drug release can be controlled with this novel aerogel-hydrogel composite system via changing hydrophobicity of the aerogel, and the concentration of the PEG in the hydrogel coating.

ÖZET

Bu çalışma sonucunda ilk defa silika aerojel ve PEG (polietilen glikol) hidrojel kompoziti sentezlenmiş ve bu yeni kompozitin ilaç taşıyıcısı olarak kullanılması araştırılmıştır. Bu kompozit, disk şeklindeki aerojellerin fotopolimerizasyon yoluyla PEG-hidrojel ile kaplanması sonucu üretilmiştir. Aerojellerin sentezinde iki basamak sol-jel metodu ve tetraetilortosilikat (TEOS) silika kaynağı olarak kullanılmıştır. Fotobaşlatıcı olarak kullanılan Eosin-Y molekülü yaşlandırma işlemi sonrasında alkojellerin Eosin-Y ve etanol solüsyonuna batırılması işlemi ile alkojel ağı içersine adsorblanması sağlanmıştır. Fotobaşlatıcı yüklü hidrofilik aerojelleri hidrofobik hale getirmek için süperkritik CO_2 fazında çözülmüş hexamethyldisilizan (HMDS) ile yüzey modifikasyonu yapılmıştır. Bu yöntem ile kontak açının 0 ile 128^o arasında değiştirildiği görülmüştür. Daha sonra aerojeller PEG diacrylate önpolimer solüsyonuna batırılmış ve 514 nm dalgaboyunda ışın ile polimerizasyon reaksiyonu başlatılarak hidrojel ile kaplanmıştır. Aerojellerinin tüm anlatılan basamaklardan sonra BET yüzey alanı ölçümü, gözenek çapı ve dağılımı ölçümleri yapılmıştır. Sonuçlar, aerojelin hidrojel ile kaplanması sırasında yapısında herhangi bir değişiklik olmadığını göstermiştir. Buna karşılık, hidrofilik aerojelin, yüzey modifikasyonu sırasında, yüzey alanının azaldığı gözlenmiştir.

Bu yeni kompozitin ilaç taşıyıcısı olarak kullanılmasını incelemek için Ketoprofen, model ilaç olarak seçilmiştir. Sonuçlar göstermiştir ki, aerojele ilaç yükleme kapasitesi ve ilacın salınımı aerojelin hidrofobik karakteri değiştirilerek kontrol edilebilinir. Aerojellerin hidrofobik özelliği artıkça, ilaç yükleme kapasitesi azalmakta ve ilacın salınımı yavaşlamaktadır. Ayrıca önpolimer solüsyonundaki polimer konsantrasyonu değiştirilerek (0, %15, %30 kütlece) ilaç salınımındaki etkisi araştırılmıştır. Polimer konsantrasyonu artıkça, ilaç salınımının yavaşladığı görülmüştür. Deney sonuçları göstermiştir ki, aerojel-hidrojel kompoziti kullanılarak ilaç salınımı aerojelin hidrofobik karakteri ve önpolimer solüsyonundaki polimer konsantrasyonu değiştirilerek sağlanabilinir.

ACKNOWLEDGEMENTS

This thesis would not have been possible without guidance and support of my advisor Professor Can Erkey. Thanks for his trust on me even when I was a senior to participate the scientific researches ongoing in his laboratory. During the last two year, I have learned many things not just about the area that I am working on, but also about the life and human being. He will always be an instructor for me with his generous, friendly, and honest character.

I would like to thank my committee members Assist. Professor Seda Kızılel for her generous encourage allowing me to use the devices and the chemical materials in her laboratory during the study and Professor Şevket Ruacan for his advice and support in my thesis work.

Special thanks to Prof. Dr. Levent Demirel and his PhD student Pınar Tatar to let me to use the device in their laboratory for the contact angel measurements.

I am indebted to many of my colleagues who supported me in any respect during the completion of the project. To Selmi Erim Bozbağ, thanks for the scientific discussions which are always make answers of the issues more obvious and also thanks for the technical assistance with easier and useful tricks. To Erdal Uzunlar, thanks for the cheerful times we had in Austria and for your support during the conference in Graz. To Caner Tatlı, thanks for your technical support and advices for the problems based on biological issues. To Nil Ezgi Dinçer, thanks for your lovely friendship during the hours we spent in the laboratory. Special thanks to Sibel Kalyoncu, Deniz Şanlı, Selimcan Azizoğlu, Enis Demir, Zeynep Ülker, Bilal Çakır, Oğuz Canıaz and also to former colleagues N. Seda Yaşar and A. Meriç Kartal to make the time I had in Koç University jovial and full of unforgettable memories.

Last but not least, thanks to my parents and lovely sister. Without you, I could not find power to finish this study. I hope that the results of this study will somehow facilitate human's life in the future and thus it will be worthwhile to all of difficulties that I had during the last two year.

TABLE OF CONTENTS

LIST OF TABLES

LIST OF FIGURES

Chapter 1

INTRODUCTION

Silica aerogels are sol-gel derived materials with high surface areas, high pore volumes and low densities [1]. They are produced by supercritical drying of the gels obtained via hydrolysis and condensation reactions of a silicon alkoxide precursor such as tetraethylorthosilicate (TEOS) in a solvent. The properties of silica aerogels can be tailored by manipulation of reaction conditions and reactant concentrations during their synthesis and they can be produced as monoliths in any shape [2]. As a result of such favorable properties, silica aerogels have been under investigation for use in many applications such as thermal insulation, dust collectors, glazing windows and particle detectors since their discovery in the 1930s [3,4]. Being environmentally friendly and non-toxic, silica aerogels can be also used in pharmaceutical industry. Their large surface area, open pore structure and tunable properties make them ideal as potential carrier materials.

Recent research efforts are being directed towards the development of use of aerogels as carrier materials for many different organic and inorganic guest materials such as PEG [5], TiO_2 [6], and Pt [7]. Aerogels are favorable due to the high specific surface area and pore volumes which influence the loading of guest material. Aerogels can be loaded basically by two methods; 1) during the sol-gel reaction [5,6] or, 2) after the drying step of the aerogels. The first method can be problematic because the guest material can interfere with the polymerization chemistry resulting in undesirable structures or can convert into undesirable products. Also, the guest material can be damaged by high pressure during the drying procedure. The second method is based on the open pore structure of the silica aerogel. Dry silica aerogels can be impregnated with molecular precursors of the guest materials from the supercritical (Sc) phase [7].

The guest material dissolved in $ScCO_2$ can be adsorbed between the pore networks of the aerogel. In this study, guest materials were loaded into the aerogel after gelation step. Eosin-Y, photoiniatior, was loaded into the alcogel during the aging step and the drug after the drying procedure from $ScCO_2$ phase.

A high purity requirement for the end product in pharmaceutical industries is the driver behind efforts to develop $ScCO_2$ based processes. In recent years, use of $ScCO_2$ as a solvent or an anti-solvent in pharmaceutical processes has been receiving increased attention. Furthermore, supercritical fluid based processes are used to micronize drugs, to extract the drug components from a wide variety of substances and to encapsulate drugs in polymeric matrices. A relatively recent field which utilizes supercritical fluid in pharmaceutical researches is the development of aerogels for drug delivery. The tunable surface and pore properties of porous silica aerogels make them promising candidates for the development of novel drug delivery devices [8, 9]. In such an approach, the drug components are dissolved in the supercritical fluid and are loaded into the porous aerogels. The method allows controlled release of drug, which can be adsorbed on a hydrophilic silica aerogel, and can be released much faster compared to its crystalline form [8]. The loading of the drug in the aerogel matrix can be controlled by the hydrophobicity of the aerogel surface which governs the adsorption isotherms.

Hydrogels have also been studied as drug delivery vehicles in pharmaceutics, biotechnology and medicine [10]. They have been prepared for use as drug carriers for the release of drugs, peptides and proteins due to their three dimensional, hydrophilic networks [11]. For example, PEG can be chemically crosslinked into hydrogels and used as reservoir devices for the controlled delivery of smaller molecular weight drugs. PEG hydrogel has received significant attention, especially because of its non-toxic, non-immunogenic and hydrophilic character. Previous studies investigated the kinetics of PEG hydrogel formation, and diffusion of various drugs and/or proteins from these PEG hydrogels [12, 13, 14]. Hydrogels can also be designed to be responsive to various properties such as pH, temperature, concentration of a metabolite or electric field which may be utilized for different applications.

In this work, a novel composite material was synthesized by encapsulation of hydrophobic aerogels within PEG hydrogel via surface initiated photopolymerization [15]. An initiator immobilized on the surface of the aerogel was utilized to start the formation of PEG diacrylate hydrogels on the surface. Eosin was used as the photoinitiator because of its spectral properties that perfectly suit its use as an initiating system for an argon ion laser [16].

The novel composite is advantageous because of the layered structure which allows many different ways to control drug release. First of all, properties such as porosity, surface area, or density of the silica aerogel can be tuned by changing the reaction conditions and hydrophobicity can also be manipulated by the technique developed. All these parameters have effect on the release rate of the drug adsorbed on aerogel from $ScCO_2$ phase. The second regulations can be made on hydrogel layer such as changing polymer concentration in the prepolymer solution or using different monomer molecular weight. As it is known, there are many methods to control the permeability or release rate of the hydrogel such as altering monomer molecular weight, concentration or using different crosslinking agents to make them responsive to the changes in the environment. The most promising aspect of the new system is the ability to carry two different drug in different layers; aerogel and hydrogel, and sequential release from them. Although, it is impossible to test all these different regulations together, we start up with two of them; tuned the hydrophobicity of the aerogel and changed PEG concentration of the hydrogel coating.

In the first part of this study, the novel composite was investigated. It is important to preserve the both aerogel and hydrogel structural properties during the synthesis. Thus, possible changes in the aerogel structure through synthesis processes were investigated by using nitrogen adsorption-desorption isotherms, BET surface area and BJH pore size calculations. As a result, two different structure such hydrophilic, wet network which is hydrogel and hydrophobic, dry network which is aerogel were successfully combined without losing their structural property. In the second part, the drug delivery application

of this composite was studied. The effects of hydrophobicity of aerogel and PEGdiacylate concentration in the prepolymer solution of the hydrogel coating on the drug release rate were examined. To test this ability, Ketoprofen (3-benzoyl-R-methylbenzeneacetic acid) was chosen as a model drug due to its well-known solubility in $ScCO_2$. Ketoprofen is widely used as non-steroidal, anti-inflammatory drug for the relief of acute and chronic rheumatoid arthritis and osteoarthritis, as well as for other connective tissue disorders and pains.

Chapter 2

LITERATURE REVIEW

2.1 Properties and application of silica aerogels

2.1.1 Synthesis and classification

Aerogel is one of the most glamorous materials since it was discovered by Kistler in 1931 [17]. It is a very light and highly transparent polymeric material. The synthesis method of an aerogel is called as "sol-gel process". During this process, organic compounds containing silica undergo chemical reactions producing silicon oxide (SiO_2). This material has many unusual properties, such as a low thermal

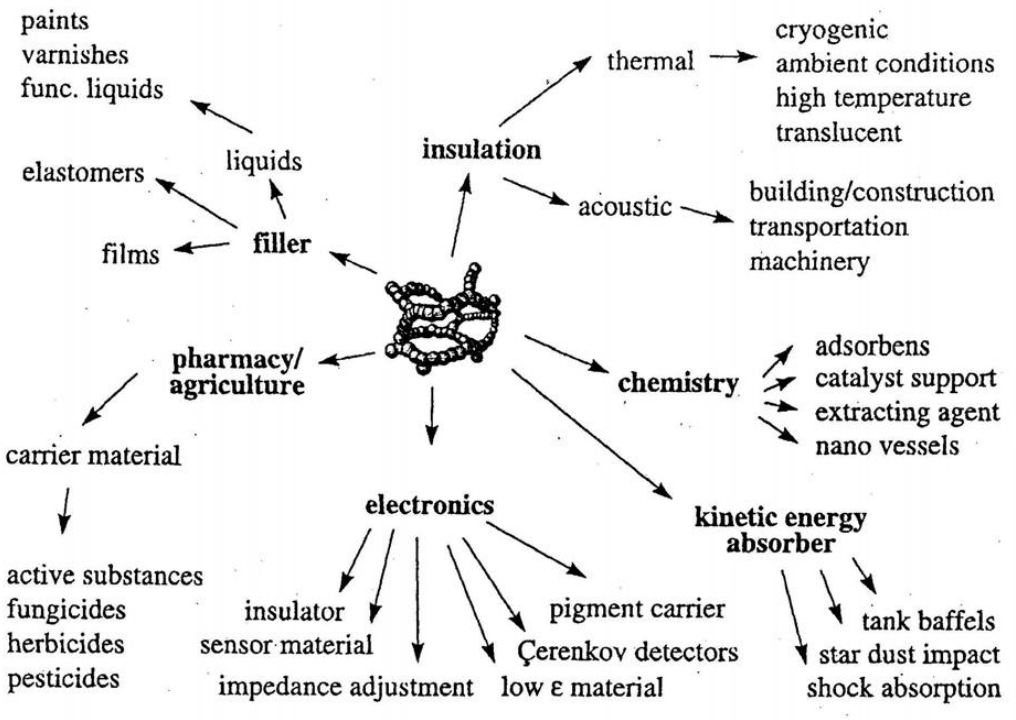

Figure 2.1 Aerogel applications [18]

conductivity, refractive index, sound speed, along with a high surface area and thermal stability (Table 2.1). An aerogel can be made with a density only three times larger than that of air. These diverse properties make aerogels applicable in many different fields of science and industry (figure 2.1).

Reactants of a silica-precursor and solvents are mixed before a reaction is started. Therefore their miscibility is important in order to prevent inhomogeneous or partially precipitated gel formation. After the reactants are fully dissolved, the solution undergoes two main reactions: 1) Hydrolysis, 2) Condensation. The kinetics of the reactions can be controlled by various parameters such as concentration of the reactants, the solvent, the catalyst used (acid catalyst or base catalyst- one step process or acid catalyst and base catalyst together-two step process), the catalyst concentration (pH value), the temperature, etc. These parameters change the properties of the resulting aerogel applicable to various fields of science and industry (figure 2.2).

• Hydrolysis:

$$\equiv Si\ OC_2H_5 + H_2O \rightarrow \equiv Si\ OH + C_2H_5\ OH \qquad (1)$$

• Condensation:

$$\equiv Si\ OC_2\ H_5 + HO\ Si\equiv \rightarrow \equiv Si\ O\ Si\equiv + C_2H_5OH \qquad (2)$$

$$\equiv Si\ OH + HO\ Si\equiv \rightarrow \equiv Si\ O\ Si\equiv + H \qquad (3)$$

The reaction mixture is a liquid at the end of first reaction, and becomes more and more viscous as the condensation reactions proceed. After some time, the solution loses its fluidity and the whole reacting mixture turns into a gel. This gel consists of a three-dimensional network of silicon oxide filled with the solvent. This form of silicon oxide is called an alcogel because the pores are filled by alcohol which was used as a solvent

in the synthesis method. During the special drying procedure, the solvent is extracted from the gel body leaving the silicon oxide network filled with air. This product is called aerogel. Indeed, if it is dried in ambient pressure and temperature, it is called xerogel (figure 2.2).

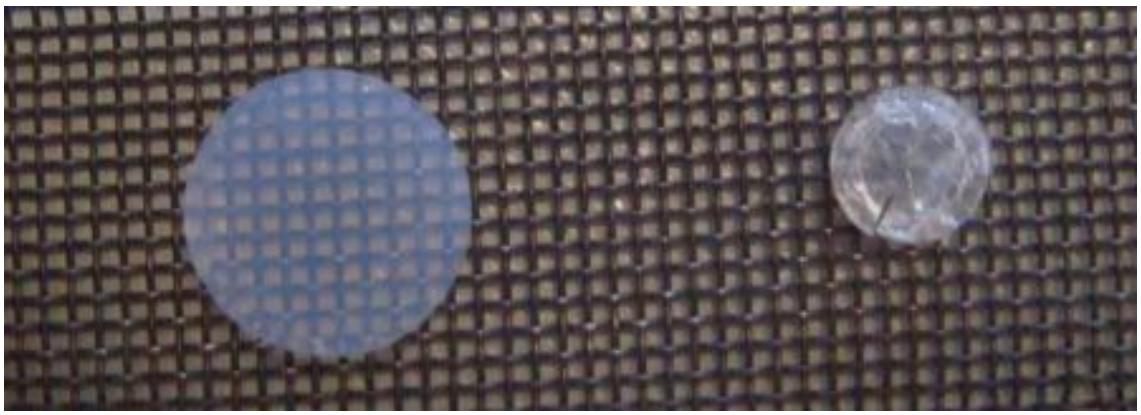

Figure 2.2 Top views of the aerogel and xerogel, respectively

Aerogels can be synthesized not only from silicon oxide (silica aerogels), but also from different organic and inorganic substances, for example titanium oxide, aluminum oxide, carbon etc [19, 20, 21].

Table 2.1 Properties of Silica Aerogel [22]

Property	Value	Comments
Density	0.003-0.35 g/cc	Most common density ~0.1 g/cc
Porosity	85-99.87 %	Open pore structure
Specific Surface Area	600-1000 m^2/g	Related to meso- or macropores range
Average pore size	~20 nm	Mostly in mesopore range
Primary particle diameter	~2-5 nm	
Transmittance	*TR* = 97.9 %	For an aerogel sample of thickness equal to 4 mm.
Thermal conductivity	0.015 W/m K in air 0.010 W / m K in vacuum	For a density of 0.15 g/cc [23].This value compares with 0.35 W /m K (in air) for polyurethanes, mineral wool and expanded polystyrene.

From figure 2.2, it can be clearly observed how drying technique changes the quality of the final product. The size difference between the xerogel and aerogel is significant. This difference is a result of the damage occurred in the pore structure of the alcogel during drying of the solvent. Ambient drying damages pore structure of aerogels due to the forces developed between the gas-liquid interface of the solvent. For instance, small droplets of mercury will form into spheres when placed on a smooth surface because the cohesive forces in the surface tend to hold the molecules together. However, molecules along the surface are subjected to a net surface toward the interior. This tensile force is called the surface tension and is designed by γ. The force created by the surface tension must be equal to the pressure difference between the internal and the external of the droplet.

Thus [24],

$$\Delta p = \frac{2\gamma}{r} \qquad (2.1)$$

It is clearly seen from this result that the pressure inside the drop is bigger than the outside. This phenomenon plays a role in the capillary rise. The same phenomenon is also valid in the pores of the aerogel. In nano-pores, capillary pressure and stress created by it can exceed the strength of the network and result in collapse of the pores (figure 2.3). Thus, shrinkage, low surface area, and cracking are the main products of the capillary pressure in the aerogel. To avoid these, supercritical fluids are used. Because above the critical temperature and critical pressure of the liquid, there is no distinction between the liquid and vapor phases i.e. the densities become equal - there is no liquid-vapor interface and, thus, no capillary pressure. This drying process is termed supercritical drying.

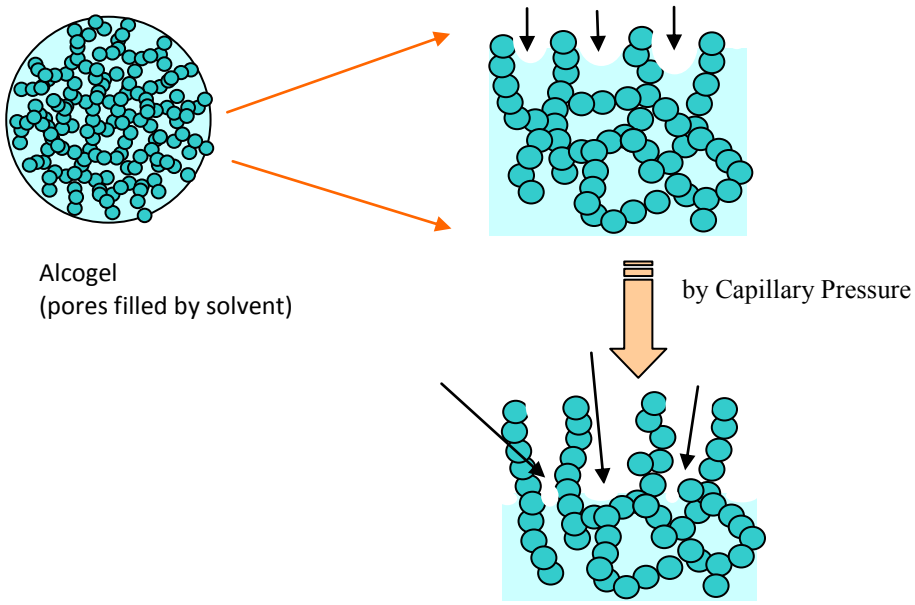

Figure 2.3 Schematic of capillary pressure effect on pore structure

2.1.2 Supercritical CO_2

A substance is defined as a supercritical fluid when it has been heated and compressed above its critical temperature and critical pressure. Above the critical temperature (T_c) and pressure (P_c) of a pure substance, we get a phase which behaves like gas and liquid at the same time [25]. The pressure temperature diagram of CO_2 can be found in the figure 2.4. Along the solid lines in this figure, two different phases are in equilibrium and in the triple point three different phases coexist. In the supercritical region there is only a single homogenous phase. Therefore, it is possible for a substance to cross from a liquid state to gas state without any phase transition by passing through the supercritical region [26].

Table 2.2 Physical properties of liquid, gas, and Supercritical fluids [27]

	Liquid	*Supercritical Fluids*	*Gas*
Density (kg/m^3)	1000	100 – 800	1
Viscosity (Pa.s)	10^{-3}	10^{-4} - 10^{-5}	10^{-5}
Diffusion Coefficient	10^{-9}	10^{-8}	10^{-5}

Density is the primary property which affects the solvent power. One of the advantages of supercritical fluids is to be able to adjust the density by simply changing the temperature or pressure of the system. Thus, supercritical fluids are used as solvent in many different applications and industries such pharmaceutics, polymer industry, textile industry etc [28]. In supercritical region, the thermophysical properties of a substance include liquid-like densities, gas like viscosities and much more higher diffusivities than liquids [27] (table 2.2).

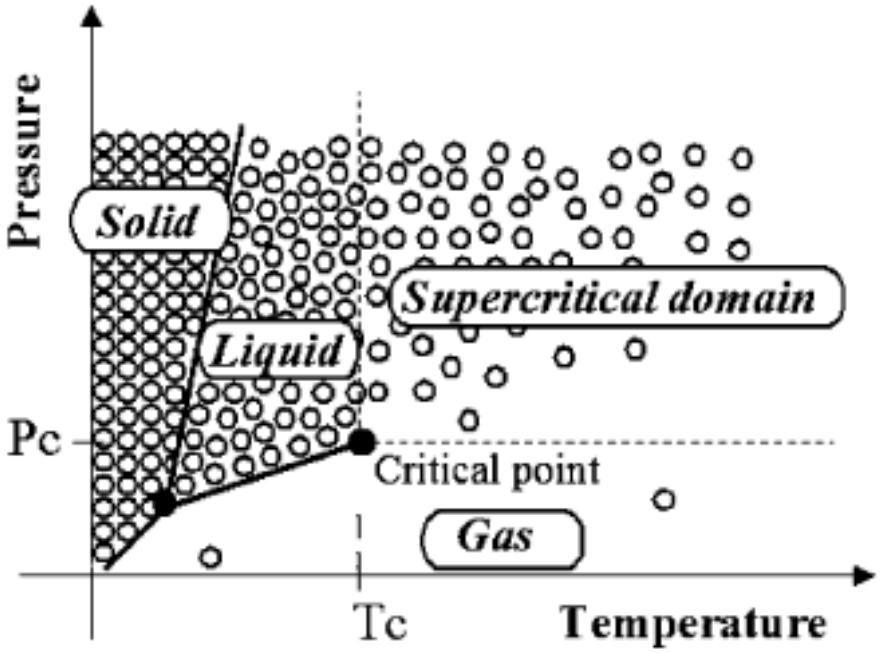

Figure 2.4 Carbon dioxide temperature-phase diagram [29]

Carbon dioxide is used in supercritical drying since its supercritical conditions are easily attainable (Tc= 304 K, Pc= 7.38 MPa) and it can be removed from a system by simple depressurization. It is non-toxic, non-flammable, chemically inert and inexpensive.

2.2 Surface and pore size analysis

As it is mentioned in the previous section, pore structure of the material depends on the drying technique used such as supercritical or ambient drying. In order to determine pore structure which is explained by the average pore size, specific surface area, shape of the pore and pore distribution of the porous material, physisorption method is used. The next section is about the details of these concepts.

2.2.1 Physisorption

Gas adsorption is a widely used method for the characterization of mesoporous materials with regard to the determination of surface area, pore size, pore size distribution, and porosity. The International Union of Pure and Applied Chemistry (IUPAC) proposed to classify pores by their internal pore width (the pore width defined as the diameter in case of a cylindrical pore and as the distance between opposite walls in case of a slit pore) [30]. According to IUPAC, the *micropore* is called to the pores of internal width less than 2 nm; *mesopore* to the pores of internal width between 2 and 50 nm; and *macropores* to the pore of internal width greater than 50 nm.

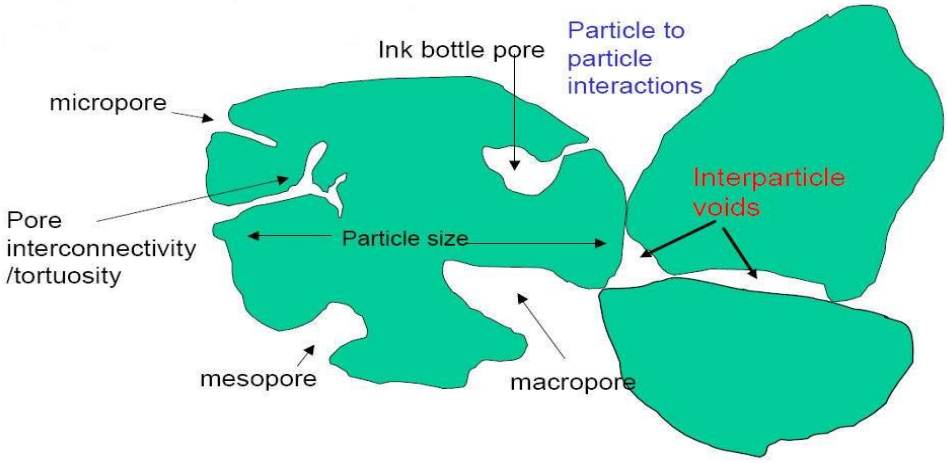

Figure 2.5 Micro, -meso and macropores [31]

Figure 2.6 shows a (schematic) sorption isotherm as it is expected for adsorption/desorption of a pure fluid in a single mesopore of cylindrical shape in combination with a schematic representation of the appropriate sorption and phase phenomena occurring in the pore. The adsorption mechanism in mesopores is at lower relative pressures (p/p_o) absolutely similar as in case of adsorption on planar surfaces. After completion of the monolayer formation, multilayer adsorption commences. After reaching a critical film thickness capillary condensation occurs essentially in the core of

the pore. The plateau region of the isotherm reflects the situation of a pore completely filled with liquid. The pore liquid is separated from the bulk gas phase by a hemispherical meniscus. Pore evaporation therefore occurs by a receding meniscus at a pressure, which is less than the pore condensation pressure. The pressure where the hysteresis loop closes corresponds again to the situation of an adsorbed multilayer film which is in equilibrium with a vapor in the core of the pore and the bulk gas phase.

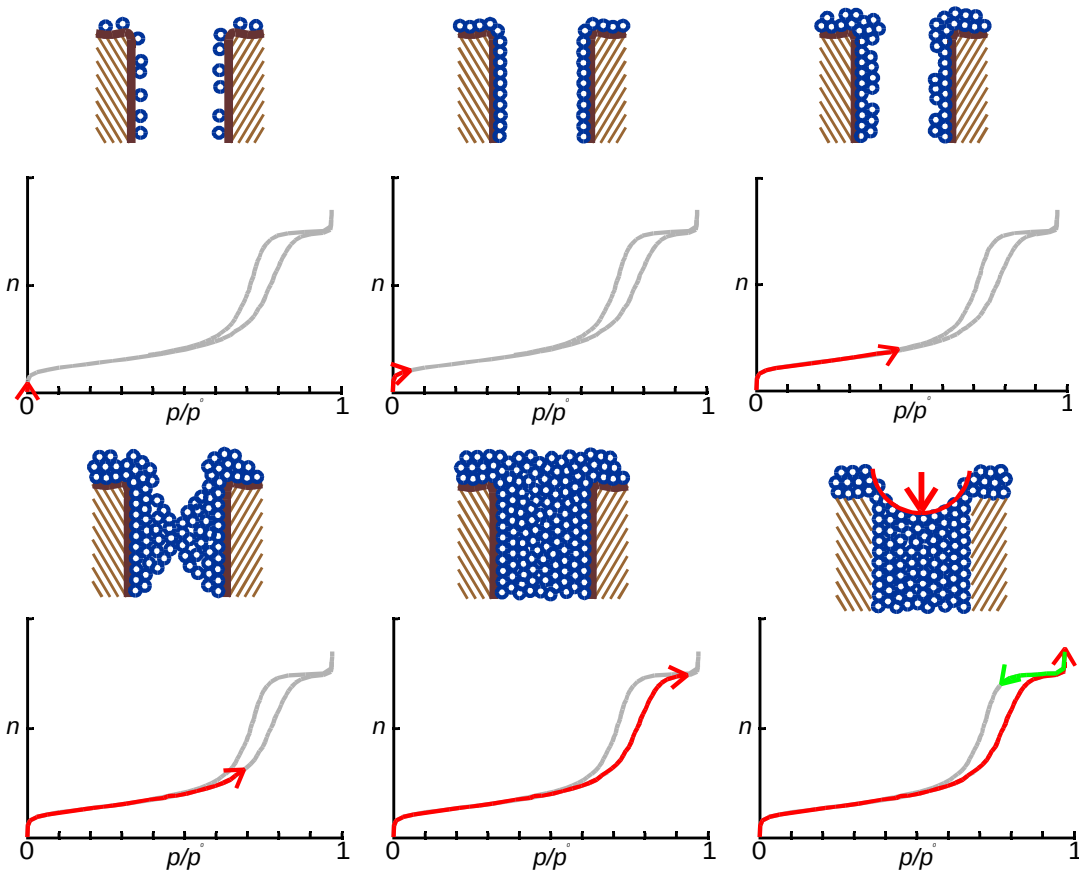

Figure 2.6 Schematic representations of multilayer adsorption, pore condensation and hysteresis in a single pore [32]

It is widely accepted that there is a correlation between the shape of the hysteresis loop and the texture (e.g., pore size distribution, pore geometry, connectivity) of a mesoporous adsorbent. An empirical classification of hysteresis loops was given by the IUPAC [30] classification is shown in figure 2.7. According to the IUPAC classification type Hl is often associated with porous materials consisting of well-defined cylindrical-like pore channels or agglomerates of compacts of approximately uniform spheres. It was found that materials that give rise to H2 hysteresis are often disordered and the distribution of pore size and shape is not well defined. Isotherms revealing type H3 hysteresis do not exhibit any limiting adsorption at high *P/Po,* which is observed with non-rigid aggregates of plate-like particles giving rise to slit-shaped pores. The desorption branch for type H3 hysteresis contains also a steep region associated with a (forced) closure of the hysteresis loop, due to the so called tensile strength effect. This phenomenon occurs for nitrogen at 77 K in the relative pressure range from 0.4 - 0.45. Similarly, type H4 loops are also often associated with narrow slit pores, but now including pores in the micropore region.

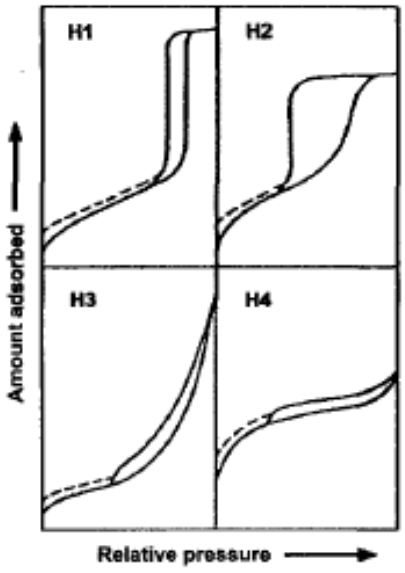

Figure 2.7 IUPAC classification of hysteresis loops [30]

As it is explained shape of adsorption/desorption isotherms and hysteresis depends on the pore size, shape and degree of disorder of the pores material. By classical Kelvin equation the relationship between the pore size and pore condensation/evaporation pressure in other words the hysteresis is explained. It uses the equilibrium vapor pressure of a liquid in the pores (p) and the equilibrium pressure of the same liquid on a planar surface (p_o).

$$\ln(p/p_o) = -2\gamma\bar{V}/rRT \qquad (2.2)$$

where γ is the surface tension of the liquid, $\bar{V}$ is the molar volume of the condensed liquid contained in the pore of radius r, R is gas constant and T is the temperature. However, classical Kelvin equation based on macroscopic assumptions, can not describe the sorption and phase behavior of fluids in narrow mesopores correctly, which leads to an underestimation of the pore size up to ca. 25% for materials consisting of pores < ca. 10 nm [33]. In narrow pores attractive fluid-wall interactions are dominant and the macroscopic, thermodynamic concept of a smooth liquid-vapor interface and bulk-like core fluid cannot realistically be applied.

On the basis of the Kelvin equation, to describe the pore condensation of uniform shape and width (ideal slit-like or cylindrical mesopores) can be described by using the shift of the gas-liquid phase transition of a fluid from bulk coexistence which is expressed in macroscopic quantities like the surface tension γ of the bulk fluid, the densities of the coexistent liquid p_1 and gas p_g ($\Delta p = p_1 - p_g$) and the contact angle θ of the liquid meniscus against the pore wall. For cylindrical pores the modified Kelvin equation [52-54] is given by

$$\ln(p/p_o) = -2\gamma cos\theta/RT\Delta\rho(r_p - t_c) \qquad (2.3)$$

where R is the universal gas constant, r_p the pore radius and t_c the thickness of an adsorbed multilayer film, which is formed prior to pore condensation. The occurrence of pore condensation is expected as long as the contact angle is below 90°. A contact angle of 0 ° is usually assumed in case of nitrogen adsorption at 77 K.

The modified Kelvin equation serves as the basis for many methods applied for mesopore analysis, including the Barett-Joyner Halenda method (BJH) [61], which is also used in our study. It provides the pore size distribution by assuming a cylindirical pore geometry.

2.2.2 Specific Surface Area

The specific surface area was evaluated using the Brunauer-Emmett-Teller method (BET) from adsorption data in the relative pressure range of 0.05 - 0.3 [34]. This range of p/p_o is suitable to evaluate the amount of the adsorbate condensed on the surface of the adsorbent in the form of a statistical monolayer known as monolayer capacity (n_m), which is necessary for calculation of the specific surface area. The monolayer capacity n_m (moles g^{-1}) can be found from the slope and the intercept of the linear form of the BET equation:

$$\frac{{}^{p}/_{p_o}}{n(1-{}^{p}/_{p_o})} = \frac{(C-1)}{n_m C}\left({}^{p}/_{p_o}\right) + \frac{1}{n_m C} \qquad (2.4)$$

where n is amount adsorbed and C is the BET constant. For n_m to be expressed in (moles g^{-1}), a unit conversion is required, namely the amount adsorbed (originally expressed in cm^3 STP g^{-1}) needs to be divided by the molar volume of adsorbate at

standard temperature and pressure (22414 cm^3 STP mol^{-1}, for an ideal gas). The conversion factors for the nitrogen at -196 ^oC are: 0.0015468.

The BET specific surface area ($S_{BET,}$ m^2 g^{-1}) is calculated using the following equation:

$$S_{BET} = n_m N_A \omega_a \quad (2.5)$$

where N_A is the Avogadro number ($6.023 \cdot 10^{23}$ molec. mol^{-1}) and ω_a is the cross- 32 sectional area of the adsorbate molecule expressed in m^2 (area occupied by N_2 at -196 ^oC is assumed to be $0.138 \cdot 10^{-18}$ m^2).

2.3 Surface Modification of Aerogels

Due to the hydroxyl groups, aerogels are highly hydrophilic. Thus, as the time passes, they can even adsorb the vapor from the air, and lose the pore structure. Decrease in surface area and pore volume cause to damage very important features of it such as thermal conductivity. In long term usage or storage of aerogels, this highly hydrophilic structure becomes a serious problem. To overcome that, many distinctive modifications have been developed by making them hydrophobic. Modification of silica surfaces can be achieved by silation of silica with hydrophobic silation agents which results in silica surfaces with hydrophobic groups. This can be achieved by replacing active hydrogen atoms on silanol by the hydrophobic (silyl) groups as shown in schematic in Figure 2.8. Bringing the silating agent in contact with the silica surface can be in vapor, liquid or supercritical fluid media depending on the phase of the solvent which carries the silating agent

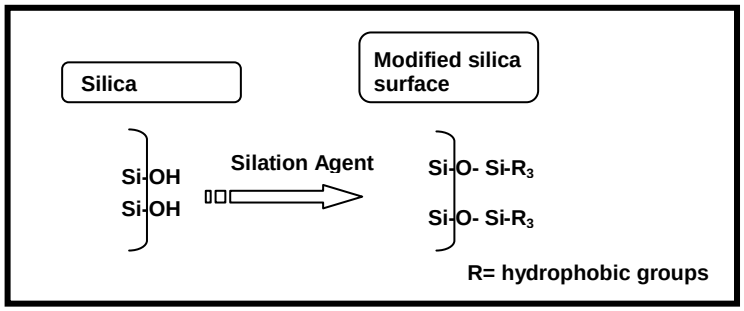

Figure 2.8 Silation of silica surface

There are mainly two different methods for the modification of the aerogels. These are Co-precursor and Derivatization methods. The next section will be about the pros and cons of these methods.

2.3.1 Co-precursor method for modification of silica aerogels

In this method, as a silica source, two compounds are used. One of them is normal silica precursor such as TEOS. However, the other one of must contain at least one non-polar chemical group such as Si-CH_3 bond. Silating agent can be the hydrophobic silation compound such as hexamethyldisilizane (HMDS) or various other organosilanes such as monoalkyl, dialkyl, trialkyl, aryl, alkoxy and chloro silanes. HMDS is a difunctional trialkyl (trimethyl) silyl silane which is known to be highly reactive with surface silanols due to the presence of highly reactive atom, nitrogen within the compound [35]. Among various organosilanes, Rao et al. found that HMDS gave the highest contact angle (135°) for aerogels synthesized using TEOS and or tetramethylortho silicate (TMOS) [36]. However, it is observed that as the mole ratio of HMDS increased, a decrease in optical transmittance from 65% to 5% and an increase in contact angle from 110° to 136°. These studies indicate that the transmittance has to be sacrificed to increase hydrophobicity for the co-precursor method. Indeed, an increase in HMDS amount causes cracks in the aerogel structure.

2.3.2 Derivatization Method

The surface modification can be made after the alcogels formed. During or after the aging step, alcogels are dipped into a mixture of a solvent (ethanol, methanol [36,35] and hexane) and SA for more than 12 hours at a temperature above 45 °C before drying. Usage of HMDS as a derivatization agent yielded silica aerogels with improved transmittance up to 70% and 88% for TMOS based and TEOS based aerogels, respectively [36]. Similarly monolithic aerogels with a transparency of 85% and a contact angle of 109° could be obtained [35]. However, ammonia can be produced by side reactions and it is difficult to remove of unreacted HMDS, ammonia and solvent by several heat treatments above 50 °C.

2.3.3 Derivatization of silica aerogels using $ScCO_2$

For silica aerogels, the methods explained above are not applicable since the large capillary forces exerted on the pores of silica aerogels when contacted with a liquid solvent lead to pore collapse. $ScCO_2$ has been attracting increased attention in modification of a wide variety of inorganic surfaces including silica due to the low viscosity, and surface tension of $ScCO_2$ coupled with adjustable properties with changes in temperature and pressure make $ScCO_2$ an attractive medium for carrying out surface modification. Furthermore, $ScCO_2$ is inert and leaves no residue on the treated surface.

In this study, the modification of silica aerogel surfaces was performed by the derivatization method using $ScCO_2$ as the solvent and HMDS as the derivatization agent [37]. As it was mentioned earlier, HMDS is found to be highly reactive with surface silanols. The modification reaction is shown in Figure 2.9.

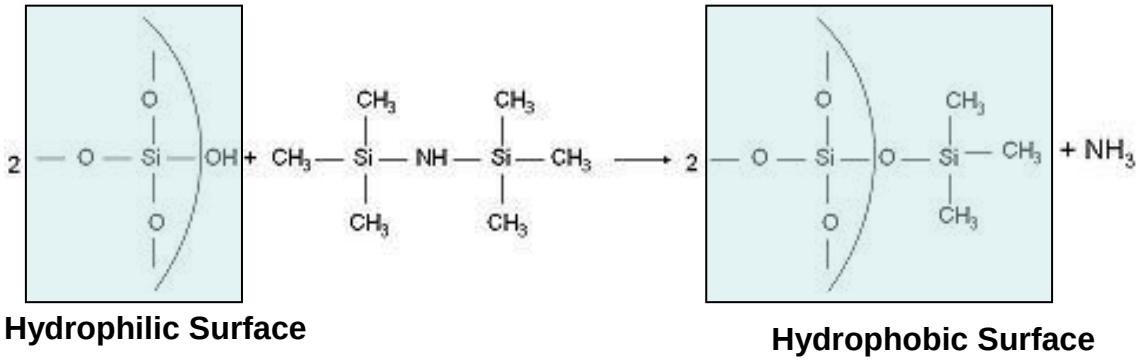

Figure 2.9 Surface modification reaction of silica aerogel with HMDS

2.4 Aerogel-Polymer Composites with Various Functions

Sol-gel-derived silica aerogel is an attractive candidate for many unique thermal, optical, catalytic, and chemical applications due to its mesoporous structure, high surface area and very low densities. However, there are many problems in commercialization because of its fragility, and highly hydrophilic structure. To overcome such challenges for silica-based aerogels, numerous attempts to strengthen the gel structure by aging, crosslinking with organic polymers, modifying surfaces hydrophobically, and conventional drying have been explored [38, 41].

In section 2.4.1, advantages of using of polymers as additives will be explained. Because drug delivery application of aerogel-PEG hydrogel composite was investigated in this study, the literature examples of aerogel and hydrogel applications in this area are of great importance for analysis of the results of this study. The next section, 2.4.2, will be about the drug delivery applications of the composites of aerogel or xerogel with or without PEG. There will be also some examples of protein delivery in which silica xerogel was used. The section 2.5 will be about the PEG-hydrogel structure and properties. Various effects such as PEG molecular weight on the permeability of the hydrogels will be examined.

2.4.1 Usage of polymers as additives to increase mechanical strength

Novak et al [38], aimed to improve the mechanical and optical property of the aerogels by incorporating the polymers into the aerogel network. In order to prevent extracting of polymers during the drying, they bind polymers to the SiO_2 network. In the first approach, polymers: poly(2-vinylpyridine) (PVP), poly[methylmethacrylate-co-(3-(trimethoxysily1)-propylmetharylate)] ~ (PMMA-TMSPM), silanol-terminated poly(dimethylsi1oxane) ~ (PDMS), were added to the sol-gel precursor solution and in the second approach poly(N,Ndimethylarylamide) (PDMA) was crosslinked to the structure in situ. Unlike PVA and PMMA, PVP shows little leaching from the gel during drying process. This is due to H-bonding between polymer and free silanol groups. The polymer- SiO_2 composite are less brittle and more ductile. Also, addition of small amounts $CuCl_2$ cause to crosslink PVP and results more mechanically strong aerogel.

Premachandra [39] and coworkers made a hybrid structure, by carrying out the supercritical drying process on composites consisting of an in situ generated silica network as the inorganic phase and a high-temperature polymer as the organic phase. A polybenzobisthiazole was chosen as additive due to its very high thermal stability, with sulfonation to increase its reactivity, and it was bonded to the silica phase by a silane coupling agent. As amount of silica used is increased, young modulus of aerogel is also increased.

Ayer and Hunt [40] used chitosan, a polymer soluble in dilute acid, as additive in silica aerogels. Chitosan is a biocompatible material that has potential for use in pharmacological, biomedical, agriculture and waste treatment products. Authors found that as chitosan weight percent increased, total shrinkage decreased from %23 to 7%, wheres B.E.T surface area was decreased from 750 m^2/g to 472 m^2/g. The decrease was attributed to the impurities in the chitosan and small portions of the polymer that did not dissolve completely.

An alternative method to supercritical drying in synthesis of nanoporous silica was mentioned by Kurumada and his co-workers [41]. They used polymer NIPAM as an additive in production of silica gel. A similar study was performed before Nakanishi and his co-workers. However, in that study they used a cross linker (BIS) which contributes to the distribution of the polymer in the silica matrix due to topological hindrance. After production step, the polymer was removed by calcination. As a result, they analyzed the consistent porous structure by nitrogen adsorption and desorption isotherms. They assumed that the porosity is determined as the volume fraction of the added NIPAM in the network of silica, that is, the pores are formed as the voids, which were initially occupied by the template poly-NIPAM chains before the oxidative removal. It is clearly shown that when polymer weight percent is increased from 0.67 to 3.0, nano-pore size is also increased from 2 nm to 10 nm. This is due to the segregation of polymers in the silica matrix. Further study was performed by Leventis and co-workers to eliminate the supercritical drying step of the polymer crosslinked silica aerogels [42]. A crosslinked aerogel soaked in pentane and subsequently re-dried at ambient pressure retains a microstructure that is practically identical to that of another crosslinked monolith that was dried with supercritical CO_2. The results suggest that the properties of crosslinked aerogels dried from pentane are very similar to those of aerogels dried using supercritical fluid extraction. The crosslinked aerogels of this study are more than 300 times stronger than the silica framework, and thus they have been able to withstand the surface tension forces during ambient pressure drying.

The mechanical effect of the polymer addition on the silica matrix was investigated by Martin et al [43]. They investigated the influence of the different concentration of PEG on young modulus of the silica aerogel. The small addition of the PEG (2.5 mg PEG/ml of sol) increased the young modulus from the 4.4 MPa to 6.5 MPa. However the further addition (10.5 mg PEG/ml of sol) of the polymer decreases monotonically the value to 0.9 MPa. As PEG concentration increased, surface area of the aerogel decreased and pore size increased that made them more opaque and white. But surprisingly, the density of the aerogel just after the supercritical drying did not change

so much with addition of the PEG. When the same measurement was taken 2 months later, the same behavior in the young modulus was observed. The small addition of PEG (2.5 mg PEG/ml of sol) increased the density from 153.3 kg/m^3 to 174.9 kg/m^3, however further addition (10.5 mg PEG/ml of sol) of the polymer caused a drop down to 147.8 kg/m^3.

2.4.2 Silica-Organic biomaterials for drug delivery

2.4.2.1 Silica xerogel – PEG composites for drug delivery

Silica and silica-organic biomaterials have great potential as drug carriers. Prokopowicz [44] prepared acid-catalyzed silica gel matrix dried at ambient conditions modified with low-molecular PEG (600) and evaluated the suitability of this matrix as a carrier material for the controlled release of the pain killer diclofenac. The release profiles from disk shaped and irregular shaped xerogel were compared. An indisputable advantage of preparation of the drug matrix is the fact that the loading efficiency of diclofenac in all matrices is close to 100%, which results from the simplicity of synthesis and lack of drug losses at the gelation step. The mean value of total drug load in the masses of disk shaped of irregular xerogels (520±12 mg) were 0.08±0.01 [%w/w] and 0.16±0.02 [%w/w], respectively. Figure 2.10 shows that the rates of drug released from pellets and irregular-shaped xerogels were followed by controlled and sustained release. However, the initial burst release was reported for the irregular-shaped xerogels. The study of the stability of PEG/silica gels in the water solutions showed that the rate of degradation followed a zero-order kinetics, irrespective of the shape, mass of xerogels, and the amount of drug used. The incomplete release of drug molecules from the PEG/silica matrices suggests that during the longer gel polymerization, a covalent bond may be formed between the entrapped reagent and the inner surface of the pores or interactions among the drug and PEG and the xerogel matrices.

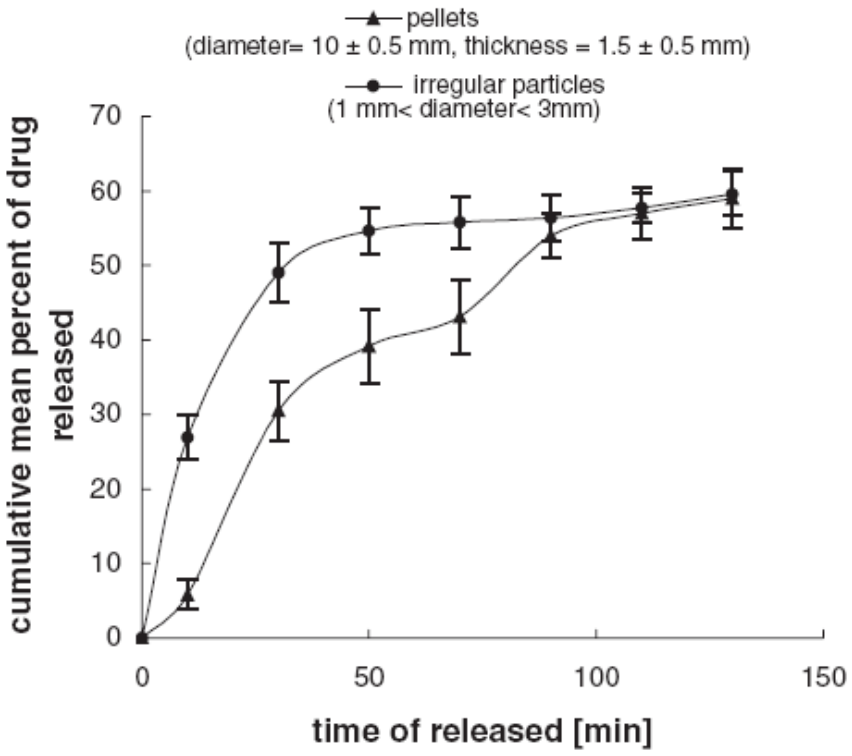

Figure 2.10 Diclofenac release from PEG/silica xerogels as a function of total time of incubation in SBF buffer solution [44]

The differences in the rates of drug released from irregular-shaped and from pellets are not statistically significant and this result suggests that the release of the drug proceeds by the same mechanism. Most likely for all PEG/silica xerogels during immersion time, a partial physical erosion of the material surface by water and/or diffusion of water molecules into the pores of the matrix took place. The release of the drug from PEG-xerogels was faster than the degradation rate of matrices, and this process was controlled mainly by its diffusion rate through the pores of the matrix. These results indicated that silica gels prepared by synthesis with low-molecular PEG can be used as an implantable drug delivery system in the different form (monolithic pellets or particles) with a controlled release.

Manja Ahola et al used silica xerogels as carrier materials for toremifene citrate in order to develop an implantable controlled release formulation for targeted and long-lasting disease control [45]. Toremifene citrate, an anti-estrogenic compound, was incorporated into silica xerogel matrixes during polycondensation of organic silicate, tetraethyl ortho silicate (TEOS). The effects of drug amount, drying temperature and polyethylene glycol (PEG) on the release rate of toremifene citrate and degradation of the silica xerogel matrix were investigated. Addition of PEG (*M*w 4600 and 10000) decreased the specific surface area of the matrix and, lowered the release rate of the drug. Reducing the amount of drug in the matrix also decreased the release rate of toremifene citrate. However, drying temperature did not affect the release rate of silica or toremifene citrate. The release profiles of toremifene citrate were according to zero order kinetics, suggested that drug release was controlled by erosion of the silica xerogel matrix. These results indicated that the toremifene citrate release rate could be controlled to some extent by adding (PEG) or by varying the amount of drug in the silica xerogel matrix. In figure 2.11, it is seen that polyethylene glycol (1.1 wt%) clearly decreased the release rate of toremifene citrate from dried (120°C) silica xerogel containing 22.9 wt% toremifene citrate. They attributed to that decrease to the small amount of PEG probably relaxes the silica network by forming larger silica capsule particles. The drug dissolved in silica sol is also encapsulated inside these larger particles and the release rate is decreased. If the concentration of PEG is high, 19 wt% or more, network formation during polycondensation is severely disturbed resulting in increased dissolution of incorporated bioactive molecules. However, the cumulative release was increased up to nearly 35 % which can be problematic in the cases high amount of drug is needed.

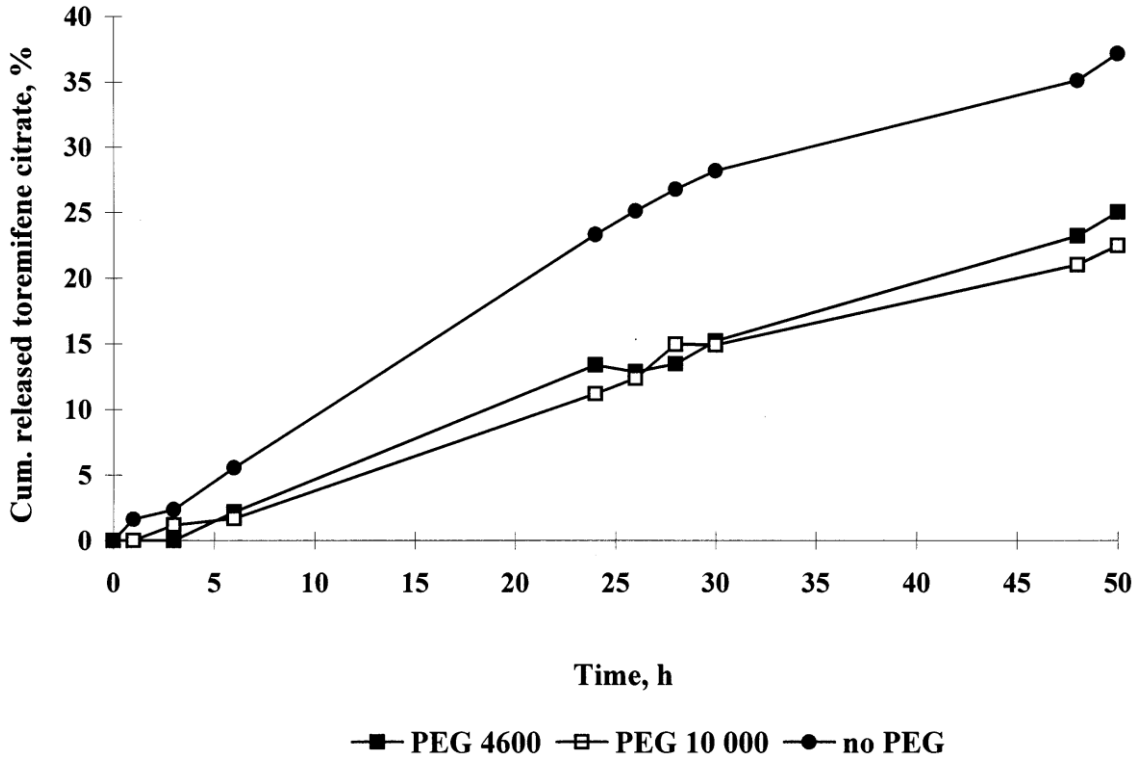

Figure 2.11 Cumulative release of toremifene citrate from silica xerogel dried at 120°C as a function of molecular weight of added polyethylene glycol [45]

2.4.2.2 Silica xerogel for protein delivery

Beside synthetic drugs, it is also possible to encapsulate proteins in the aerogels. Proteinase K was the model drug for the study of the Winny Dong et al [46]. In that study it was encapsulated in aerogel, xerogel. The protein release and the specific activity were measured. It was found that the specific activity of the Proteinase K encapsulated in the aerogel was significantly (>60%) lower than that of xerogels. This result can be attributed to the supercritical drying procedure, surface chemistry, or solvent interaction.

The potential of wet sol–gel derived silica gels as new matrices for the entrapment and sustained release of proteins was investigated in the study of Deborah Teoli et al [47]. Model proteins, BSA, ribonuclease-A and avidin, with differing molecular weights, were entrapped in two silica polymer formulations having different silica contents (4% and 12% wt/v). The conformational stability of the proteins after entrapment and their release after immersion into physiological conditions were measured. Results showed that protein conformation is maintained after entrapment and stability is enhanced. Embedded proteins maintain their original conformation and are stable to both thermal denaturation and protease degradation. Gels are highly erodible, as demonstrated by both *in vitro* and *in vivo* experiments. No local or systemic toxicity was observed after subcutaneous administration in mice. *In vivo* experiments did not show any inflammatory response around the site of injection of the 4% gel, thus suggesting that the material is well tolerated and does not induce immune system stimulation. Protein release was demonstrated to occur due to both diffusion and matrix erosion. The relevance of each of these two phenomena varied with each formulation. At low silica concentration, erosion was the driving element; at higher concentrations differences between individual proteins were observed. These data indicated that wet silica polymers obtained by the sol–gel route are promising matrices for the sustained release of protein drugs.

The paper by Erick M. Santos et al [48] describes the synthesis and protein release profiles of silica sol-gel derived materials used as carriers for a model protein that approximates the size of bone growth factors. Trypsin inhibitor (TI) was chosen as the model protein because its size (21 kD) is similar to that of bone growth factors and it has been used in similar studies evaluating polylactic acid (PLA) carriers. Over an immersion duration of nine weeks the cumulative TI release varied between 20 and 40%, depending on the original TI amount in xerogels (figure 2.12). This form of protein release is advantageous for applications that require biomolecule release duration of weeks for the full biological effect to be realized. The faster 1st-order release is related to the increase in pore size and pore volume, as this facilitates

diffusion of proteins through the porous structure of the xerogels. The in vitro release experiment was designed such that the degradation of the xerogels would be impeded and, thereby, would not affect protein release.

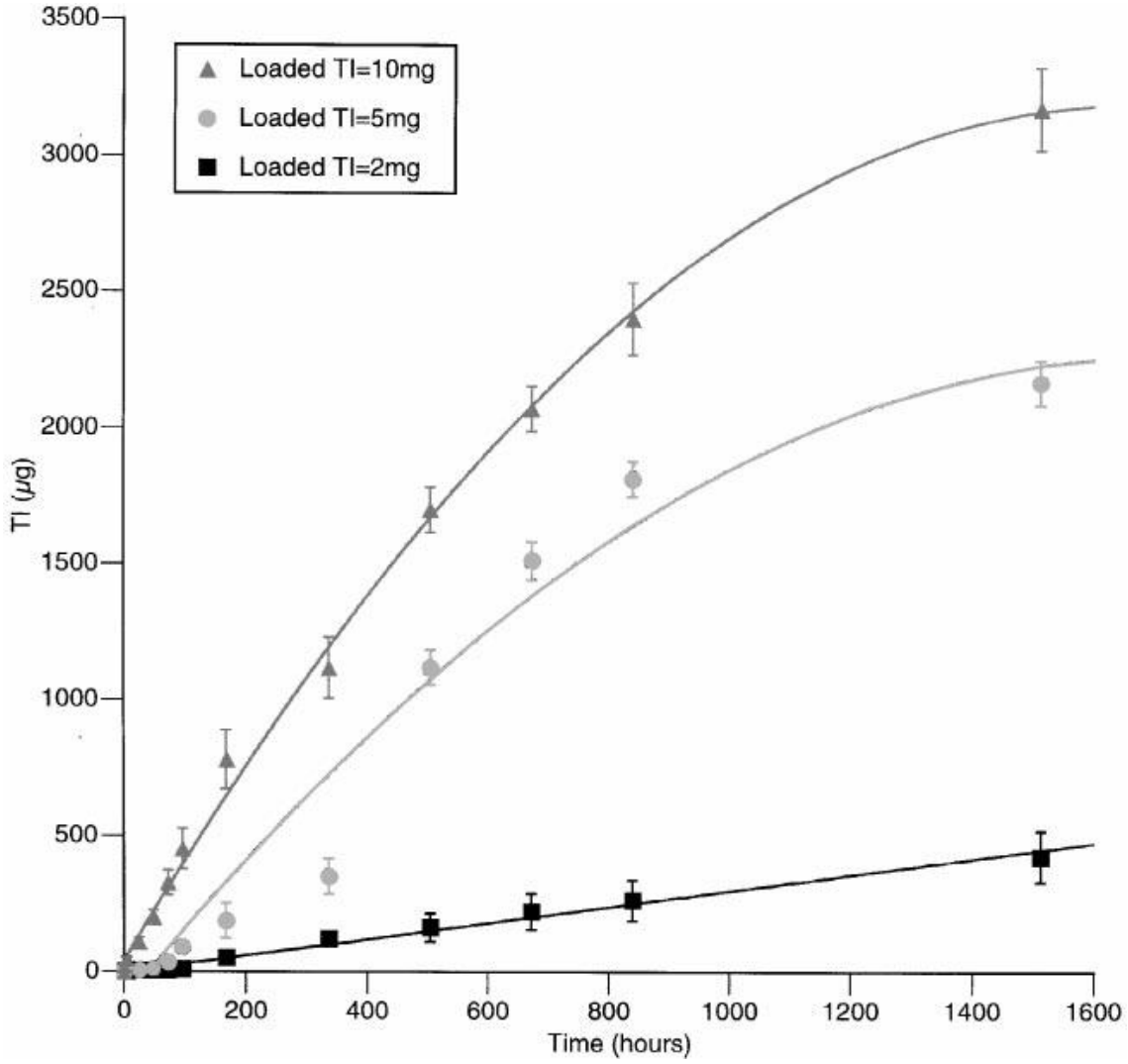

Figure 2.12 Cumulative TI release from TI-2, TI-5, and TI-10 xerogels as a function of immersion time up to 1512 h (9 weeks). After 9 weeks of immersion the total TI release from the TI-2, TI-5, and TI-10 xerogels was 21.2, 43.4, and 31.8% of the original protein content [48]

The experiment was designed this way such that protein release would not follow from carrier degradation, but would rather be the result of a diffusion-controlled mechanism. Notwithstanding this analytical goal, it is very well possible that in vivo behavior of the xerogels may differ from the conditions of this experiment. Actually, degradation of the silica matrix of these carriers can occur in vivo due to the continuous flow of fluids past the carrier surfaces.

2.4.2.3 Silica aerogels for drug delivery

Beside all applications of xerogel in drug delivery, aerogels are more promising material for this approach due to the its highly porous structure. Smirnova et al used aerogels as drug carriers [8, 49, 50]. Silica aerogels were loaded with several drugs by adsorption from their solutions in supercritical CO_2. It was demonstrated that for all three drugs (ketoprofen, griseofulvin and miconazole) investigated, high loading of the drug could be achieved. The release profiles of two drugs (ketoprofen and griseofulvin) from loaded aerogels were measured. It was found that the drugs adsorbed on hydrophilic silica aerogels dissolved faster than the corresponding crystalline drugs. This fact was explained by both an increase in the specific surface area of the drug adsorbed on the aerogel and its non-crystallinity in this state (figure 2.13). The influence of density and hydrophobicity of aerogels on both the adsorption and release of drugs were studied. The loading of aerogels with drugs depends on different process parameters such the concentration of the drug in the bulk phase (supercritical CO_2), which is limited by the solubility of drugs in supercritical CO_2, and chemical structure of the aerogel. It is seen that the adsorption of ketoprofen on hydrophobic aerogel is lower than on the hydrophilic aerogel of the same density. This difference can be explained by the lack of polar –OH groups on the surface of hydrophobic aerogels.

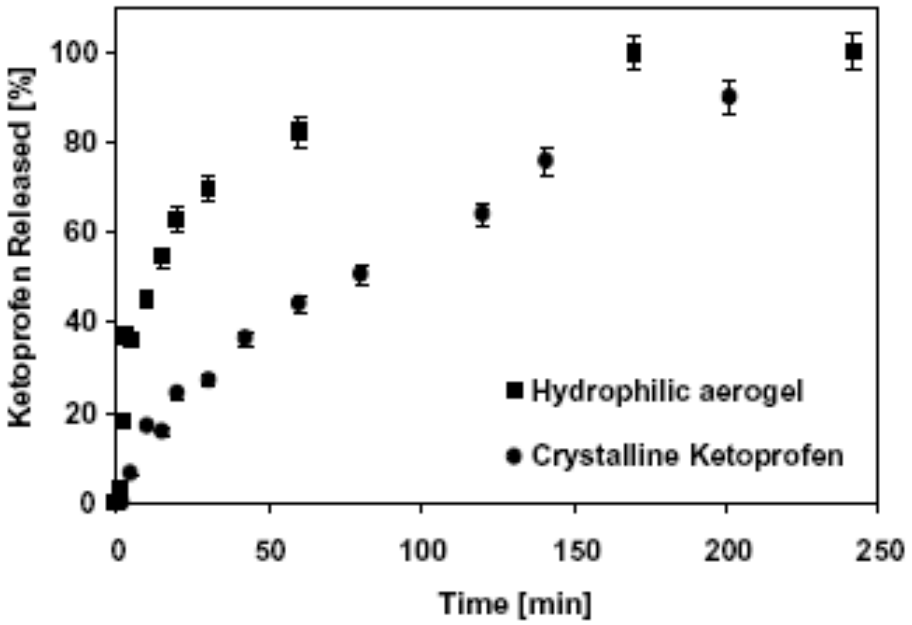

Figure 2.13 Release kinetics of ketoprofen [49]

The release of drugs from drug-loaded aerogels depends on the nature of the drug itself and on the properties of the carrier-aerogel. It was demonstrated that the use of hydrophilic aerogels as a carrier promotes fast release of the drugs. This effect can be explained by both an increase of specific surface area of the drug adsorbed on the aerogel and its non-crystalline structure in this state. In the case of the crystalline drugs, even with a very small particle size, the crystals should be destroyed before the drug can be actually dissolved. If the drug is adsorbed on the aerogel, this step is eliminated and the dissolution process is accelerated [49, 50]. Another important effect is the erosion of aerogel structure in water. Hydrophilic silica aerogels rapidly adsorbed water molecules due to the hydrophilic nature, so the drug molecules are surrounded with water allowing a fast dissolution of drugs. If the same drug is adsorbed on hydrophobic aerogels, its dissolution becomes slower (figure 2.14). At the beginning of the dissolution process, the drug dissolves from the surface of the aerogel and then later

diffuses from its pores. Because the structure of hydrophobic aerogels is much more stable in water than that of hydrophilic samples, the release process from hydrophobic aerogels is governed to a greater extent by the slower influx of water, which leads to a slower release. Thus both the loading of silica aerogels with drugs and their release rate can be influenced by the properties of silica aerogels.

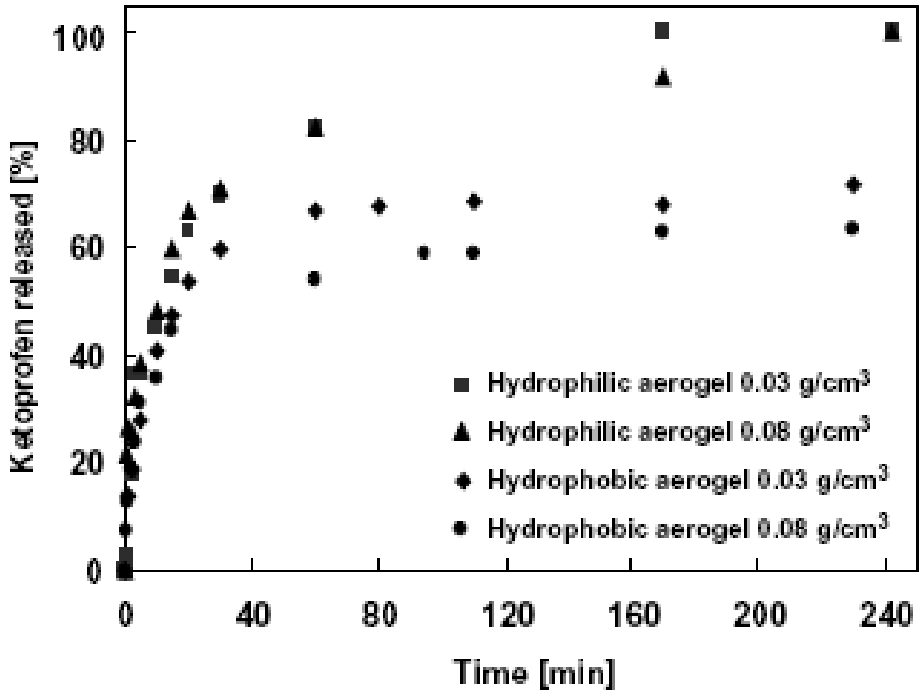

Figure 2.14 Release of ketoprofen from hydrophilic and hydrophobic aerogels of different densities

In this study, for hydrophobization of the aerogel, methanol vapor was used. Hydrophilic silica aerogels were placed in a reactor and heated to 220 ^{o}C. Methanol vapor was passed through the reactor for 13–40 h. The authors claimed that the resulting aerogels were extremely hydrophobic but did not give the exact value such as contact angle of the aerogel surface.

2.5 PEG-Hydrogels as a Drug Carrier

In the previous sections, examples of silica aerogels in drug delivery application were explained. However, in this study aerogel and hydrogel composite system was used for drug delivery. Thus, it will also be worthwhile to mention about examples of the hydrogel applications in that area.

Biocompatible polymeric hydrogels are extensively used for biomedical/ pharmaceutical applications such as controlled drug release and delivery, tissue engineering, and regenerative medicine. While various methods of gelation (i.e., physical, ionic, or covalent interactions) can be used to form PEG gels, chemically or covalently-crosslinked gels leads to relatively stable hydrogel structures with tunable physicochemical properties such as permeability, molecular diffusivity, equilibrium water content, elasticity, modulus, and degradation rate [51] (figure 2.15). The water content can be up to 95 % for loosely crosslinked hydrogels. This high water content makes hydrogels very similar to natural tissue and hence, creates suitable environment for biomolecules and cells. In tissue engineering, cells such as pancreatic islets or human stem cells can be encapsulated by PEG- hydrogels to protect them from degradation, or the attack of immune system [56]. Also, degradable hydrogels especially increases its potential when it is used as cell delivery scaffolds. The ability to control the degradation rate is critical for the tissue regenerative applications [52].

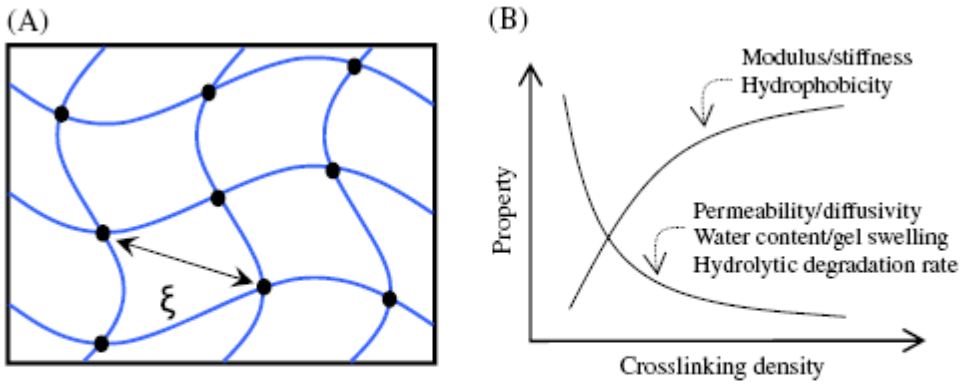

Figure 2.15 A) Simplified crosslinked hydrogel structure. Black dots represent crosslinking point; ξ represents mesh size of the gel. **B)** Hydrogel property as a function of gel crosslinking density [52]

The design criteria for the PEG-based hydrogels are that the delivery of the right dosage and the preserving of the molecular bioactivity. One way to control the release kinetics is to tune the crosslink density of the hydrogel. The porosity of hydrogel which depends on the crosslink density affects the diffusion coefficient of the drug in the hydrogel, and thus determines the release rate of drug. Another effective way to control the release rate from the hydrogels is to design them as a "smart" hydrogels which are responsive to the changes in the pH, temperature and ionic strength. These responsive hydrogels can switch from a collapsed to swollen state. Under appropriate stimulus, drugs encapsulated in the hydrogels are released in the swollen state.

The other challenge is to preserve the bioactivity of the molecules during and after the loading procedure. For example, when proteins or nucleic acids are encapsulated in the PEG-Hydrogels during radical-based hydrogel crosslinking, the highly reactive free radicals or undesired reaction can damage the biomolecules.

In addition to these, new techniques have been developed for synthesizing aerogels from the hydrogels without destroying their porous structure [53, 54, 55]. Alginates, carrageenans, and chitosans were used to convert hydrogels into aerogels [53]. The

drying procedure prevented extensive damage to the porous structure of the hydrogels. This procedure involved immersion of the hydrogel microspheres in a series of consecutive solutions of alcohol in water, with increasing alcohol concentrations up to 100%. The dehydrated, but alcohol soaked spheres, are dried at 31.58 in supercritical CO2 at 74 atm. The average pore size of the aerogel were 38 nm, 19 nm and 11 nm and surface areas are 570 m^2/g , 200 m^2/g , 330 m^2/g respectively. Freeze drying was another method to convert hydrogels to aerogels [54, 55]. In this method cellulose acetate derived hydrogels were used. Aerogels prepared by them were highly porous and their density was low (0.02 g/cm^3). These investigators expected that such aerogels will find a variety of medical and pharmaceutical applications for tissue engineering, drug delivery, separations, etc.

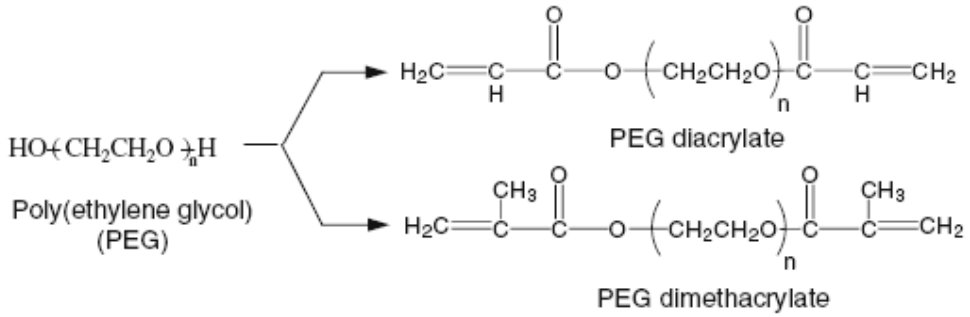

Figure 2.16 Chemical structures of PEG macromer and its di(meth)acrylate derivatives that often solution polymerize to form hydrogel networks useful for cell encapsulation and other biomaterial applications

The effect of crosslinking density was investigated by varying molecular weight and concentration of the dimethacrylated PEG macromers (figure 2.16). Alternation in PEG gel crosslinking density decreased the available free volume in the matrix for the movement of the molecules such as proteins and drugs [56]. Thus, the release kinetics

could be tuned by changing the crosslink density. The size or molecular weight of the compound which diffuses through the hydrogel are factors which affect permeability. For example, the diffusion coefficients of high molecular weight compounds; myglobin, ovalalbumin, albumin and IgG are not the same with that of lower molecular weight components such as vitamin B_{12}.

The effect of PEG diacrylate molecular weight and concentration on water content of the hydrogels, number average molecular weight between crosslinks, M_c, and mesh size are shown in Table 2.3. Significant difference was observed for the value of M_c. It differs for different PEG diacrylate molecular weights at constant PEG diacrylate concentration. By comparing the M_c and mesh size values, we can say that the permeability of these hydrogels were not equal to each other. For instance, all PEG 2K based hydrogel is permeable for vitamin B_{12} but not for big molecules such as myglobin, ovalalbumin, albumin and IgG . However, all PEG 20K hydrogels permeable for B_{12} and also for myglobin [57].

Table 2.3 The effect of PEG diacrylate molecular weight (ranging from 2K (MW: 200) to 20K (MW: 20 000)) and concentration on the network strucure of PEG diacrylate hydrogels [57]

	Water Content	M_c (g mol^{-1})	Mesh Size ($\dot{A}$)
10% PEG 2K diacrylate	84% ± 4%	150 ± 85	14 ± 6
20% PEG 2K diacrylate	84% ± 3%	277 ± 91	19 ± 5
30% PEG 2K diacrylate	83% ± 2%	337 ± 53	21 ± 3
10% PEG 4K diacrylate	87% ± 2%	302 ± 121	22 ± 5
20% PEG 4K diacrylate	83% ± 2%	355 ± 98	22 ± 4
30% PEG 4K diacrylate	84% ± 4%	530 ± 235	27 ± 8
10% PEG 8K diacrylate	90% ± 1%	538 ± 119	31 ± 4
20% PEG 8K diacrylate	87% ± 2%	738 ± 185	34 ± 6
30% PEG 8K diacrylate	82% ± 2%	494 ± 92	25 ± 3
10% PEG 20K diacrylate	93%±2%	1961 ± 1566	70 ± 38
20% PEG 20K diacrylate	91% ± 1%	1666 ± 413	58 ± 10
30% PEG 20K diacrylate	87% ± 3%	1138 ± 389	42 ± 10

The effect of molecular weight of the drug and polymer concentration on the release rate can be seen from figure 2.17 [58]. The release diagram of different molecular weight of fluorescein isothiocyanate(FITC) labeled dextrans as macromolecular model drugs from hydrogel indicates that the diffusivity changes with the molecular weight of the drug (20 kDa, 150 kDa and 2000 kDa molecular weigths). The difference between the two polymer concentrations (5% and 10%) was generally very small. However, higher polymer concentration such as 30 % could give better results in the aspect of controlled release. As the release is getting slower, the amount of total drug released is also decreased. Thus, the studies show that the release from PEG based hydrogel can be adjusted by considering different factors such as the necessary drug amount for special cases and the molecular weight of the drug.

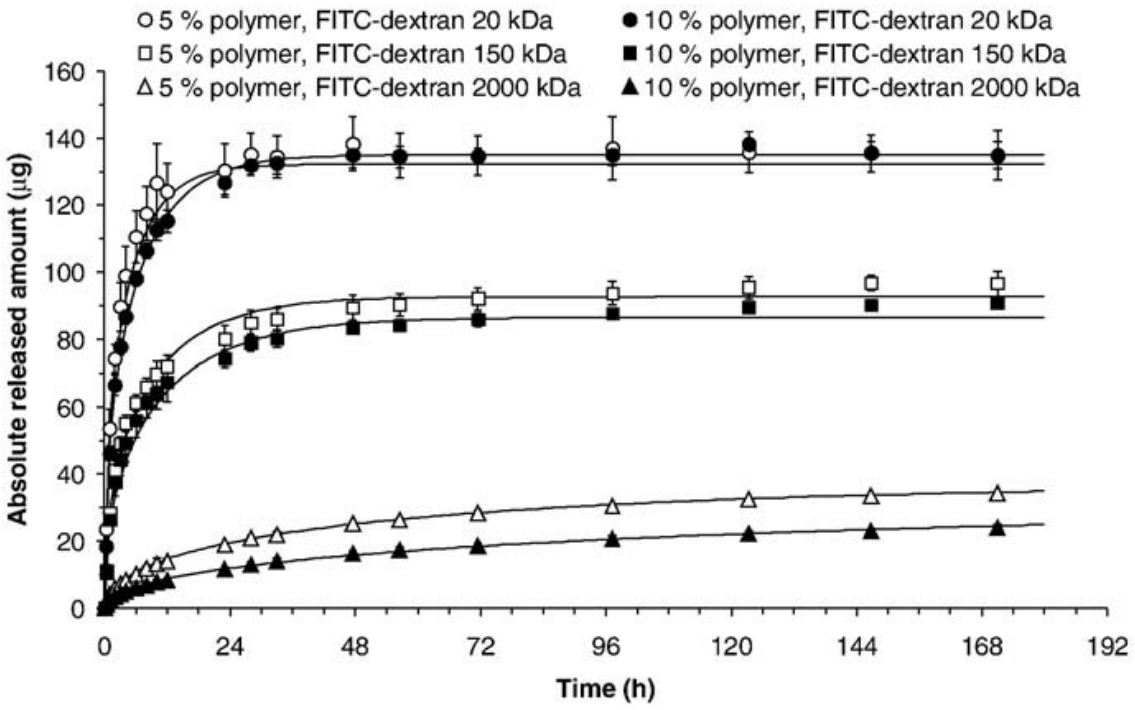

Figure 2.17 Absolute cumulative amounts of released FITC-dextrans

Chapter 3

EXPERIMENTAL SECTION

3.1 Synthesis of Silica Aerogel

Silica aerogels were synthesized by a two-step procedure using tetraethylorthosilicate (TEOS) (from Aldrich with 98.0% purity) as the precursor, HCl (from Riedel-de Haen with 37% purity) as the hydrolysis catalyst and NH_4OH (from Aldrich 2.0 M in ethanol) as the condensation catalyst. A 50 wt. % solution of TEOS in ethanol (from Merck with 99.9% purity) was prepared. Subsequently, water and acid catalyst were added to start hydrolysis under continuous stirring. Condensation started with the addition of the base catalyst and the sol was taken into cylindrical molds with a diameter of 10 mm for complete gelation (figure 3.2-a). The overall molar ratio of TEOS: Water: HCl: NH_4OH were kept constant at 1: 4: $2.44x10^{-3}$: $2x10^{-2}$ respectively. These mole ratios were kept constant in the aerogel synthesis. The typical amounts of each compound for synthesis of a sample of silica aerogel are shown in Table 3.1.

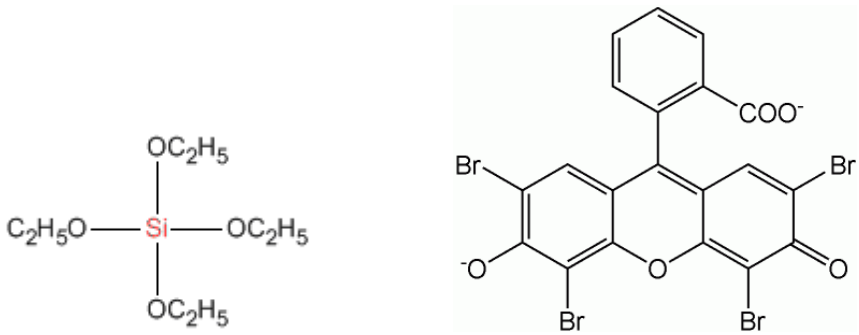

Figure 3.1 Chemical Structure of TEOS and Eosin-Y respectively

Table 3.1 Compounds in the synthesis of silica aerogel

Compound	Amount added in sol	Remarks
TEOS	1 g	Correspond to 0.0048 moles
Ethanol	1 g	50 wt. % solution of TEOS and Ethanol is obtained
Water	0.34 g	Correspond to 0.0189 moles
0.05M HCl/Ethanol Solution	0.2 ml	Correspond to $9.6.10^{-6}$ moles of HCl and 0.003 moles of ethanol. The sol at this step is left for hydrolysis for 40 minutes.
0.1M NH_4OH / Ethanol Solution	0.5 ml	Correspond to $5.0.10^{-5}$ moles of NH_4OH

After gelation was finished, the alcogels were taken out from the mold and placed in an aging solution which was 50 vol. % ethanol and water, and left in furnace at 323.2K for 20 hours. The aim of the aging step was to improve the mechanical strength of the alcogel. Next, the alcogels were kept for three more days in pure ethanol in order to remove all the impurities other than ethanol (figure 3.2-b). After aging step, they were contacted with 2mM eosin-Y, a photoinitiator, in ethanol solution. The adsorption of eosin-Y on the surface of alcogel led to a reddish transparent composite of silica alcogel with eosin-Y (figure 3.2-c). The alcogels with eosin-Y were subsequently dried by supercritical CO_2 ($ScCO_2$) at 313 K and 10.3 MPa (figure 3.2-d). The disk shaped aerogels which were obtained were hydrophilic.

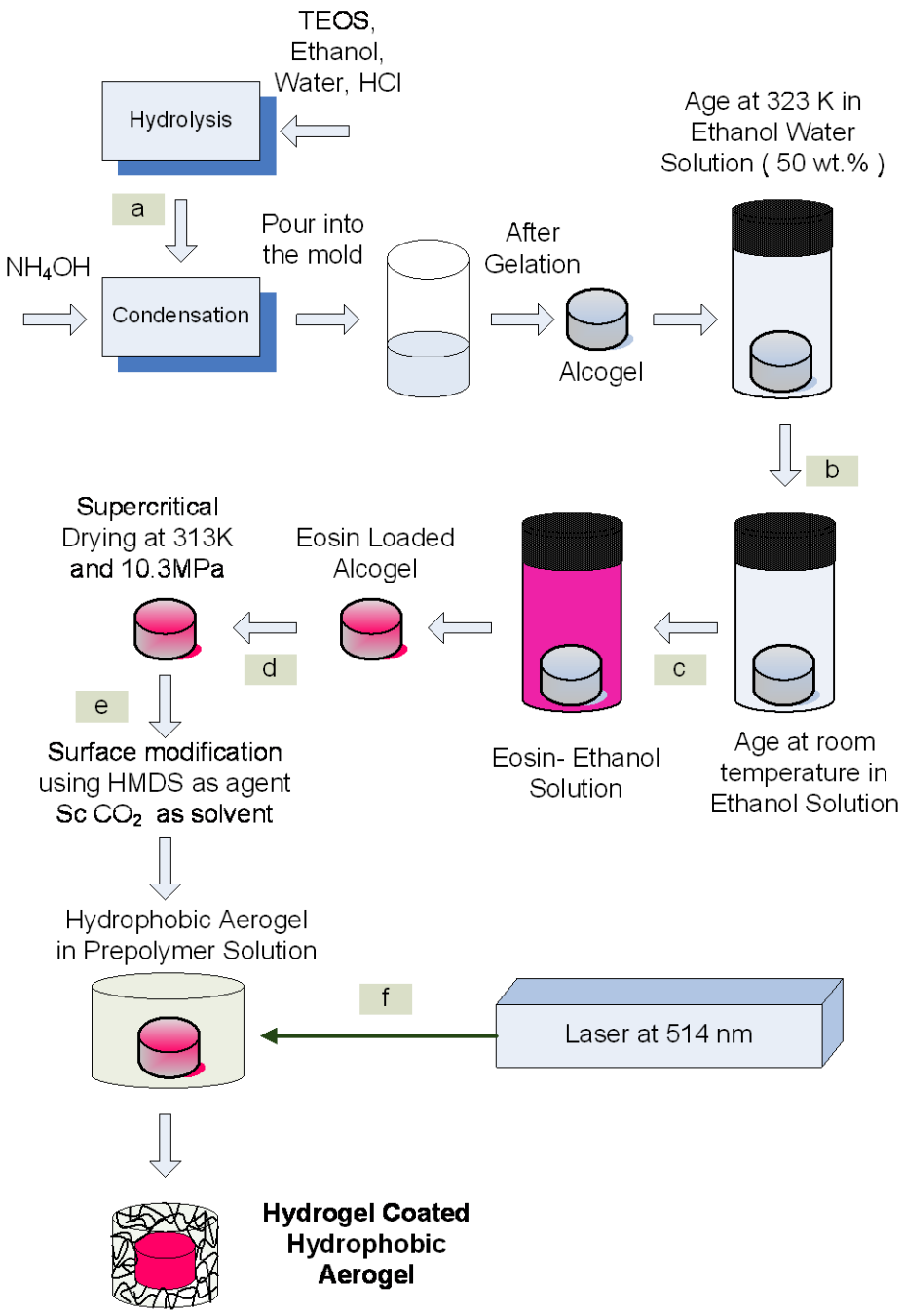

Figure 3.2 Schematic representation of the overall synthesis

3.2 Apparatus and Procedure for Surface Modification of Silica Aerogels

The experimental apparatus for the surface modification of hydrophilic silica aerogels can be seen in figure 3.3. Two high pressure vessels were used for conducting our experiments. One of them was used as the reaction vessel. It had an internal volume of 54 ml and two sapphire windows for viewing the contents. The other one with a volume of 25 ml was used for mixing HMDS with CO_2. For a typical experiment, a certain amount of hydrophilic silica aerogel sample was placed in the reaction vessel and the vessel was brought to a temperature of 333.2 K by circulating water using a circulating heater (Cole-Parmer polystat temperature controller). The vessel was then charged to 10.34 MPa with CO_2 using a syringe pump (Teledyne ISCO model: 260D) and isolated at these conditions. The mixing vessel was prepared by placing a known amount of HMDS into the vessel within a glass vial along with glass beads which kept the glass vial intact and the vessel was charged with CO_2. This vessel was also kept at 10.34 MPa at ambient temperature for 48 hours until all the HMDS was dissolved in CO_2. The surface modification of the hydrophilic aerogels was achieved by the injection of HMDS from the mixing vessel to the reaction vessel. This was realized by pressurizing the mixing vessel up to 20.68 MPa by charging with CO_2 from the syringe pump. The CO_2 – HMDS mixture at 20.68 MPa and at room temperature was injected into the main vessel by opening the valve between the reaction vessel and the mixing vessel. This procedure was repeated until the reaction vessel reached also 20.68 MPa. The vessel was isolated at 20.68 MPa and at 333.2 K for the reaction of silica aerogel surface with HMDS for 30 min. After the reaction, the extraction of excess HMDS and other reaction byproducts was carried out at 10.34 MPa and at the reaction temperature. Then the vessel was depressurized at the same temperature and modified samples were obtained after the vessel was cooled. The surface modification reactions were carried out by changing ratio of HMDS/Aerogel (w/w) in $ScCO_2$. The ratio was rendered from 0 to 4.2 during this study.

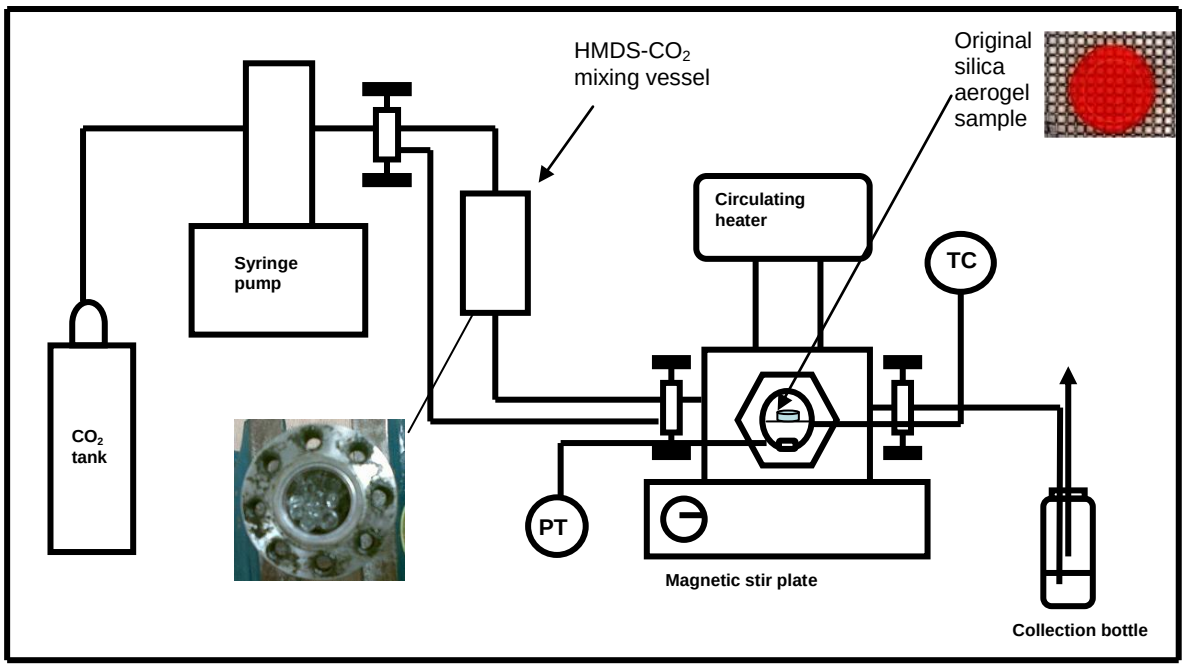

Figure 3.3 Apparatus for surface modification of hydrophilic silica aerogels

3.3 Characterization of Treated Silica Aerogels

3.3.1 Contact Angle Determination

Contact Angel measurements were done in the laboratory of Prof. Dr. Levent Demirel. The instrument was a home-made device which included a camera connected to a computer. By the help of the special program in the computer, the contact angle measurements were performed successfully. First of all, 2 μl or 3 μl of water was taken by the micro-pipette, droplet was added on the top the aerogel surface and placed in front of the camera. After taking a picture of this image, the angle between the water droplet and surface was measured by set-squared ruler (figure 3.4). For each surface, the measurement was done more than three times and the average of these measurements was taken as a final value.

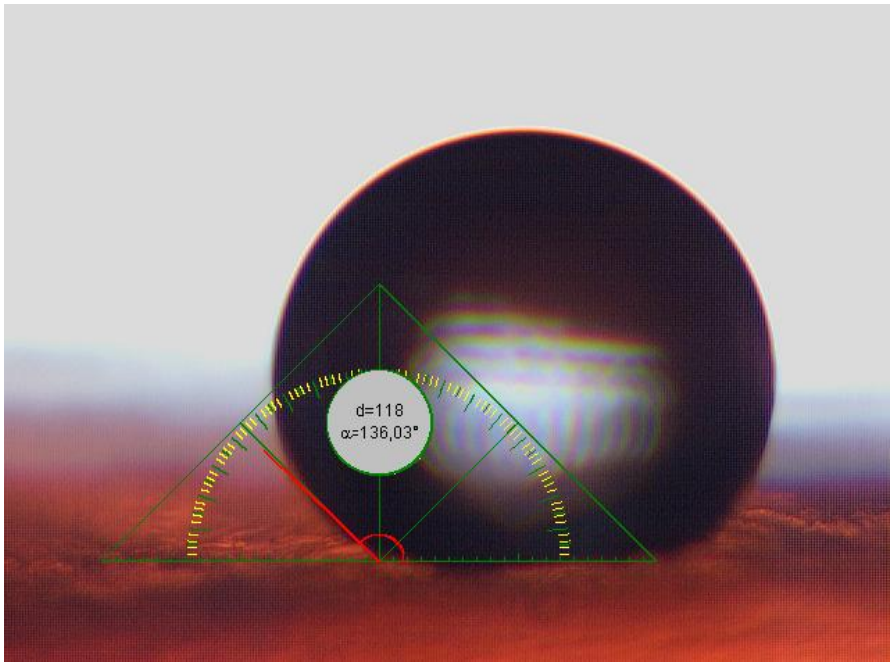

Figure 3.4 Image of the droplet on the aerogel surface

3.3.2 Pore structure analysis done with nitrogen adsorption-desorption measurements

The effects of the eosin loading and the surface modification step on the pore structure of the aerogel were investigated with the adsorption/desorption isotherms of nitrogen at 77 K by Micromeritics ASAP 2020 surface analyzer. Each sample was degassed at 573 K for at least 150 minutes before the analysis. For the hydrogel coated aerogels, in order to separate hydrogel from the aerogel, before the analysis they were left at the furnace at 323 K. As the water evaporated from the hydrogel, the shrinkage of the hydrogel layer occurred and the dry polymer separated from the aerogel surface without damaging the aerogel. The resulted pieces of the aerogel were used in the pore structure analysis.

3.4 Deposition of the Ketoprofen on Silica Aerogel

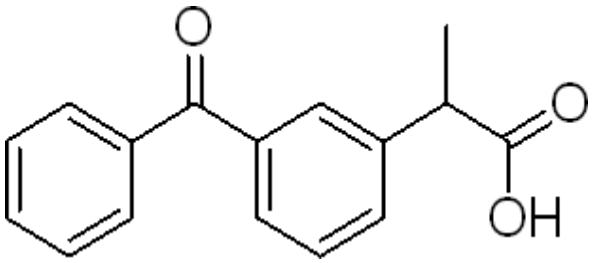

Figure 3.5 Structural formula of *Ketoprofen*

A weighted amount of Ketoprofen (from Sigma-Aldrich) and aerogel was separately placed in the vessel. After the vessel temperature reached 333 K, carbon dioxide was added until the pressure was 22 MPa. The system was kept under this condition and constant stiring for 48 hours to reach the adsorption equilibrium. The CO_2 was vented and the loaded aerogels were weighted. For all loading experiments in $ScCO_2$, ratio of the mass of aerogel to the mass of Ketoprofen was kept constant as one. The concentration of the drug was chosen so that the bulk CO_2 phase was saturated with the drug. Also, it was found that aerogel density affected the drug loading capacity of the aerogel. Thus, it was again kept constant as 0.2 g/cm^3 to eliminate that variable. The amount of loaded drug was calculated by taking the difference of the aerogel mass before and the after loading procedure.

Table 3.2 Physical Properties of ketoprofen

M, g/ mol	254.29
$T_{Melting}$, ^oC	94
Solubility in water, mg/ 100 mL	18.5

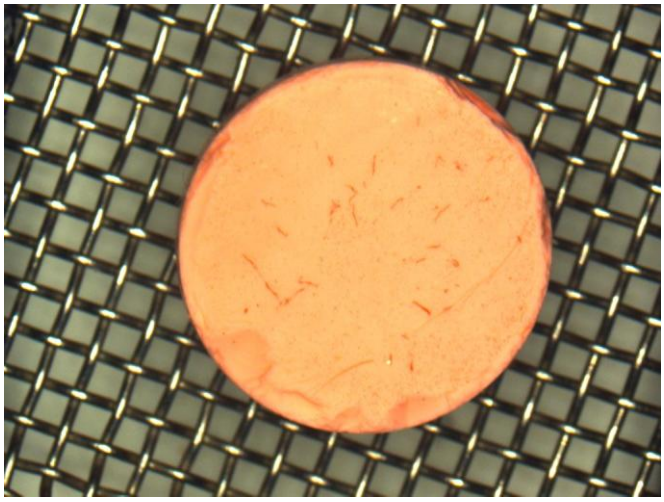

Figure 3.6 Top view of the ketoprofen loaded hydrophilic aerogel

3.5 Hydrogel Coating of Silica Aerogels

The hydrogel precursor was prepared with concentrations of 225 mM triethanolamine, 30% and 15% (w/w) PEG diacrylate (MW = 575 Da), and 37mM 1-vinyl-2-pyrrolidinone (NVP). The solution was adjusted to approximately pH 8 using 6 M HCl. Precursor solutions were filter sterilized using a 0.2 μm syringe Teflon filter. Eosin and drug loaded hydrophobic or hydrophilic aerogels were immersed in PEG-diacrylate prepolymer solution and photopolymerization was carried out using visible light (514 nm) for 3 min for each surface of the aerogels (figure 3.2-f). Immobilized initiator on the triplet state of the eosin dye produces an eosin anion radical and a triethanolamine cation radical. This is followed by rapid proton loss from the triethanolamine radical cation ($TEA^{\cdot+}$), resulting in a neutral α-amino radical ($TEA^{\cdot}$), which is generally assumed to initiate free-radical polymerization [16-59]. This step resulted in the formation of a crosslinked thin PEG hydrogel coating through surface-initiated polymerization around the hydrophobic or hydrophilic aerogels.

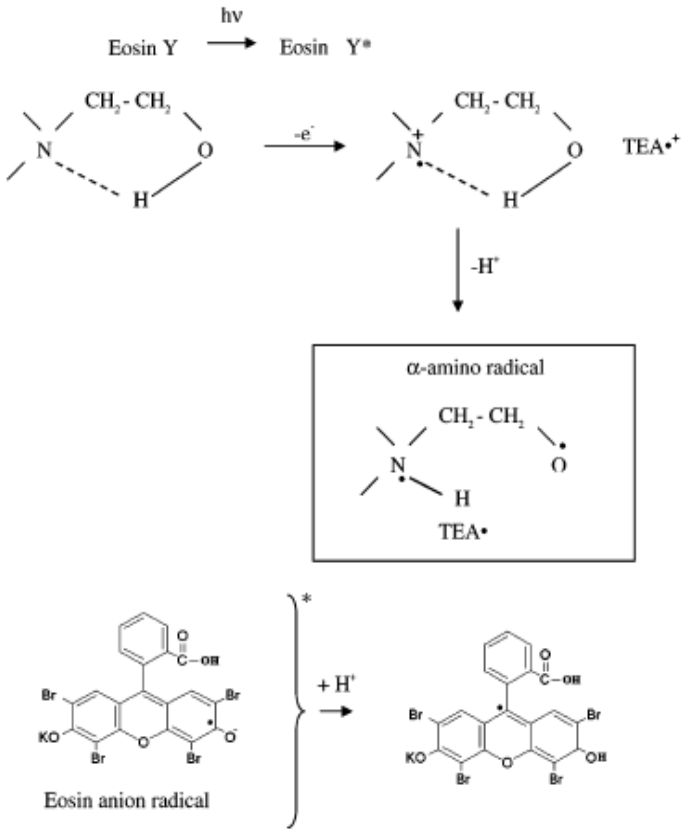

Figure 3.7 Schematic Representation of the Photoinitiation Process [15]

3.6 Ketoprofen Release Experiments

Drug release experiments were conducted at 310 K and under constant string at 100 rpm. The release medium was selected as 0.1 N HCl solution. Each aerogel sample was covered with a filter paper bag and immersed into a glass vessel containing 100 ml 0.1 N HCl solution. The glass vessel was covered and put onto a stirrer which was placed into the furnace at 310 K. At specific time periods, approximately 20 µl samples were taken using a micropipette (Eppendorf). Nanodrop spectrophotometer (Thermo Fisher Scientific Nanodrop 1000 spectrophotometer) was used to measure the concentration of the drug in these samples taken during the release experiments. The characteristic peaks of Ketoprofen were detected at 260 nm wavelength. The calibration curve can be found in the Appendix-1.1.

Chapter 4

RESULTS AND DISCUSSION

4.1 Functionalization and Coating of Silica Aerogel

Prior to ketoprofen loadind step, silica aerogels were modified twice before the drug loading step during Eosin-Y loading and HMDS treatment. Because of these modifications, aerogel's nanoporous structured may be disturbed and lose the some of the pores. Thus, it is crucial to investigate the changes in pore structure of the aerogel.

Even by naked eye, some physical information about the effect of modifications on the aerogels can be reached. It is observed from figure 4.1-a and 4.1-b that the colorless transparent aerogel obtained a red color due to the presence of eosin within the aerogel structure. The figure also shows that eosin molecules were homogeneously distributed throughout the aerogel. After surface modification step, hydrophobicity of the aerogel was verified by placing a water droplet and measuring the contact angle on the surface of the aerogel (figure 4.1-c). The contact angle for the eosin modified hydrophobic aerogel was found to be 128^{o}. Figure 4.1-d shows the image of a PEG hydrogel coated eosin functionalized hydrophobic aerogel. The thickness of the hydrogel coating was approximately 0.3 mm.

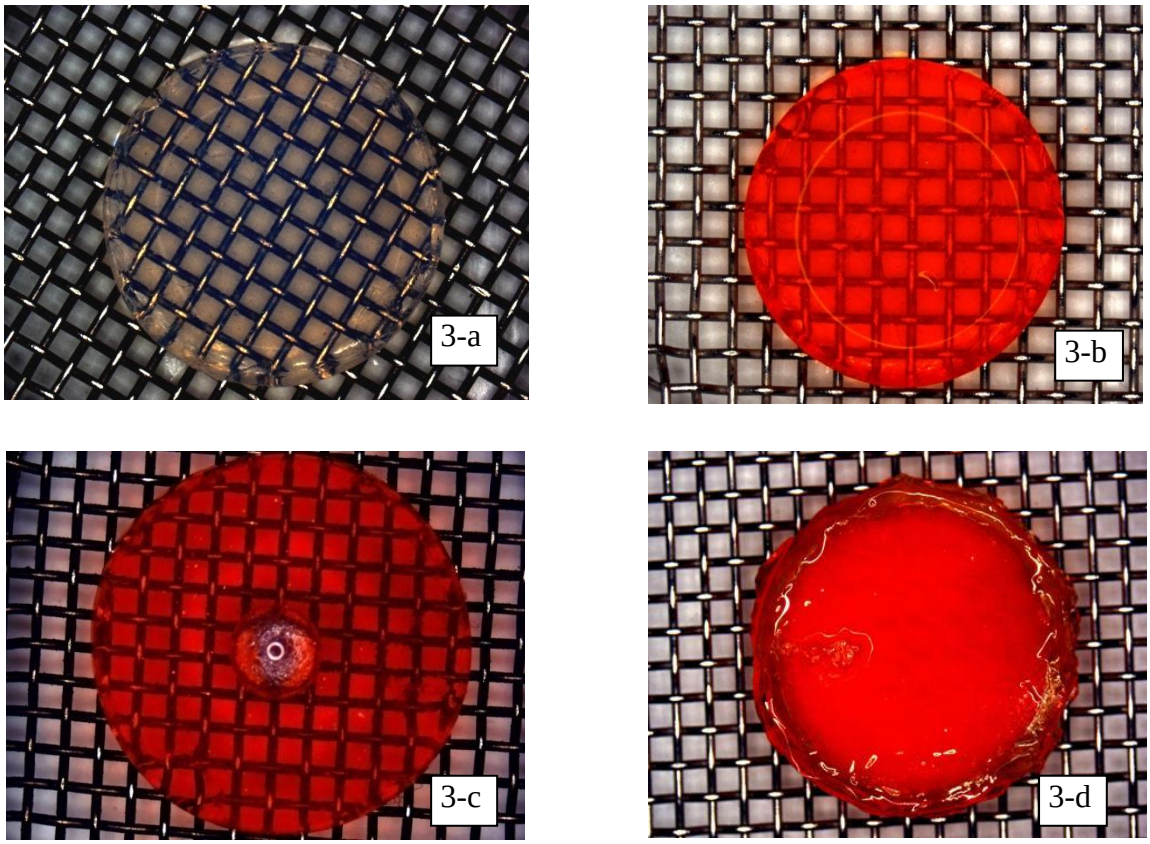

Figure 4.1 a) Image of the pure aerogel, **b)** Image of the Eosin doped hydrophilic aerogel, **c)** Image of water droplet on the Eosin doped hydrophobic aerogel, **d)** Image of the hydrogel coated hydrophobic aerogel

The effects of eosin loading and surface modification step on the pore structure of the aerogel were investigated with the nitrogen adsorption analysis. As seen in Table 4.1, the presence of eosin on the aerogel surface caused the BET surface area to decrease slightly with no appreciable changes in the average pore diameter. Further modification of the eosin functionalized aerogel surface with HMDS decreased the cumulative pore volume, surface area and also increased the average pore size slightly. This can perhaps be attributed to the presence of some bottleneck type pores which are blocked by Si-$(CH_3)_3$ groups which are results of the surface modification reaction. The

adsorption isotherms and pore size distributions of modified aerogels are compared in Figure 4.2-a and 4.2-b. All samples exhibited similar pore size distribution and type H1 isotherm which indicates that the materials consist of compacts agglomerates of approximately uniform spheres of silica and such a network is not disrupted by eosin loading, surface modification, and PEG hydrogel coating.

Table 4.1 Change in Pore Structure of Aerogel after Each Step in Synthesis

	BET Surface Area	BJH Desorption Cumulative Pore Volume	BJH Desorption Average Pore Radius
Pure Aerogel	926 m^2/g	2.9 cm^3/g	5.9 nm
Eosin Loaded Aerogel	820 m^2/g	2.5 cm^3/g	6.0 nm
After Surface Modification	528 m^2/g	2.1 cm^3/g	6.4 nm
After Hydrogel Coating	529 m^2/g	2.2 cm^3/g	6.7 nm

BET surface area and pore size distribution measurements were carried out for both non-coated and coated aerogels. The data showed that the surface area of the hydrophobic aerogel did not change after encapsulation with PEG hydrogel. Also, the isotherms and pore distributions of the two samples were nearly identical which indicate that the hydrogel coating was only restricted to the external surface of the monolithic disks and the water based prepolymer solution

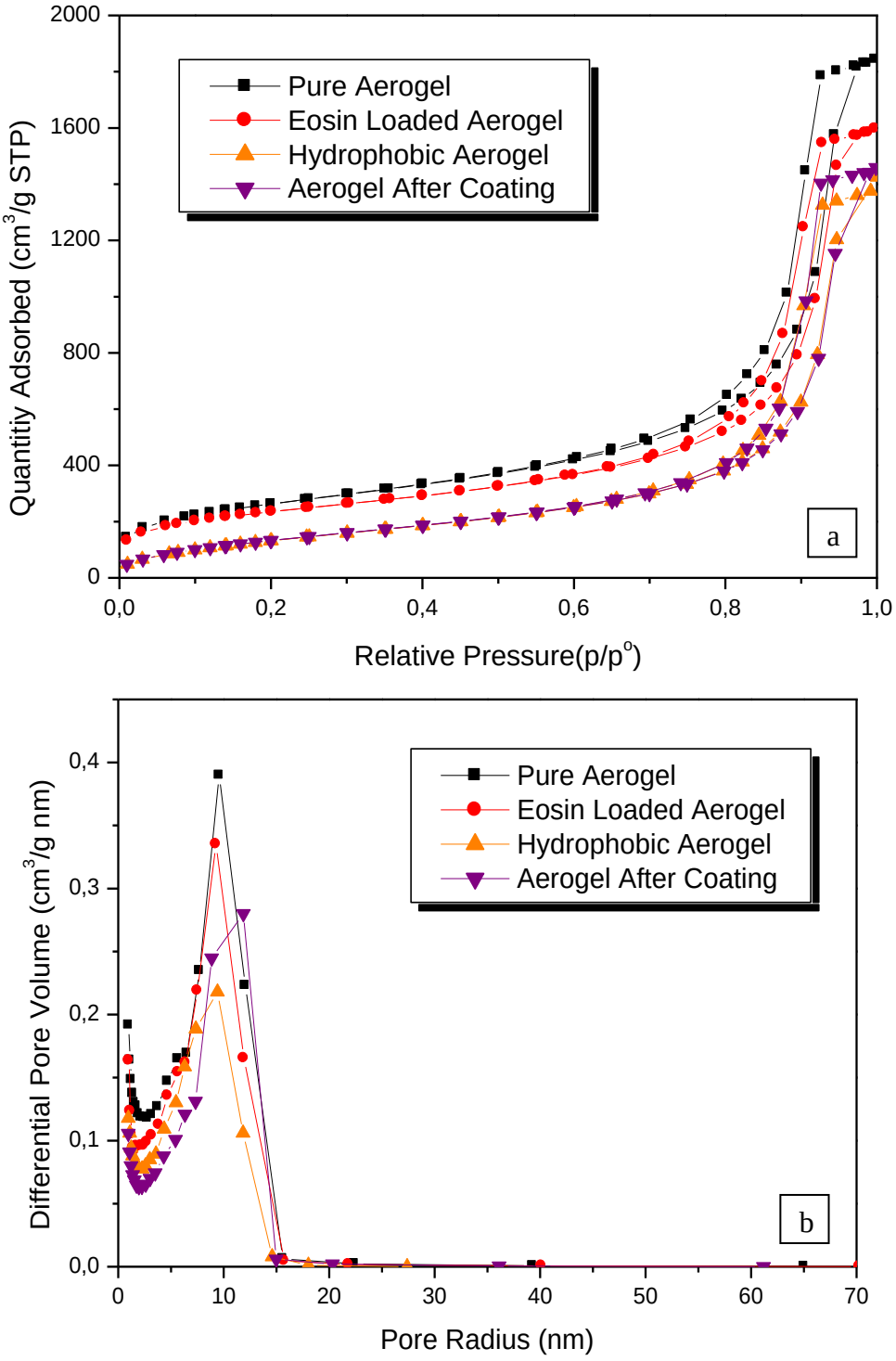

Figure 4.2 a) Effect of eosin loading and surface modification on nitrogen adsorption**, b)** Effect of eosin loading and surface modification on pore size distribution

4.2 Characterization of Hydrophobicity and Ketoprofen Loading Capacity

There are mainly two methods of loading aerogels with drug or proteins. These are loading from supercritical phase or addition of drug during the sol-gel synthesis. Second one is problematic because the drug can interfere with the polymerization reaction during the sol-gel synthesis and be trapped into the silica particles. The first one is more favorable because in that case, supercritical CO_2 was used as solvent which is non-toxic, and can be easily removed from the media during depressurization process. As model drug, Ketoprofen was chosen because there are many studies in the literature about its solubility in $ScCO_2$. Its solubility at 331.5 K and 22 MPa is $15.5*10^{-5}$ mol % [60].

In addition to these, studies of Smirnova et al. shows that the adsorption isotherm of Ketoprofen strongly depends on hydrophobicity of silica aerogel. The loading of the hydrophobic aerogel is lower than that of the hydrophilic aerogel which is explained by the lack of OH groups, which provides the active sites for the hydrogen bonding in the case of hydrophilic aerogel. Our results are in good agreement with those already described in the literature (Table 4.2) and indicate that as a result of hexamethyldisilazane (HMDS) modification aerogels become hydrophobic that affect both drug loading capacity and also release rate. Indeed, the promising side of that method is to enable us to control hydrophobicity of aerogel. This is a further advantageous for controlling the drug release.

During HMDS modification step, the ratio of HMDS/aerogel (mg/mg) in $ScCO_2$ was critical to render the phobicity of the aerogel, as the hydrophobicity was produced as a result of the reaction between the OH groups of aerogel and $Si(CH_3)_3$ groups of HMDS. Therefore decreasing or increasing the amount of HMDS in $ScCO_2$, provides a control in the number of moles of OH groups on the surface of aerogel. It should be noted that we obtained gradient in hydrophobicity in the disk shaped aerogels, when lower amounts of HMDS was used, which resulted in higher hydrophobicities at the outer surface compared to the core of the aerogel. This is due to the fact that the

reaction between OH groups and $Si(CH_3)_3$ groups starts from the outer surface of the aerogel and moves towards the core of the aerogel. In order to determine the effect of the ratio of HMDS/aerogel (mg/mg) in $ScCO_2$ on drug loading and the degree of hydrophobicity of aerogels, aerogels with different HMDS/aerogel (mg/mg) in $ScCO_2$ ratios were prepared. The results showed that, as the ratio was increased from 0 to 4.2, hydrophobicity was also increased from 0 to 128^o (further increase in that ratio did not increase hydrophobicity further), while drug loading capacity decreased from 96 to 7 % (w/w) (Table 4.2). These percentages correspond to 41 mg and 4 mg total drug amount, respectively. It should be noted that tuning of the hydrophobicity of the aerogels allowed us to control the release of the drug, and made it possible to synthesize aerogels with specific contact angels (figure 4.3).

Table 4.2. Results of contact angle and drug loading of different hydrophobic aerogels

Ratio of HMDS/Aerogel (mg/mg) in $ScCO_2$	Contact Angle	Mass Percentage of Drug Loading to the Aerogel Mass
0	**0**	**96**
1.1	**0**	**-**
1.8	**66**	**25**
2.3	**87**	**13**
3	**128**	**-**
4.2	**128**	**7**

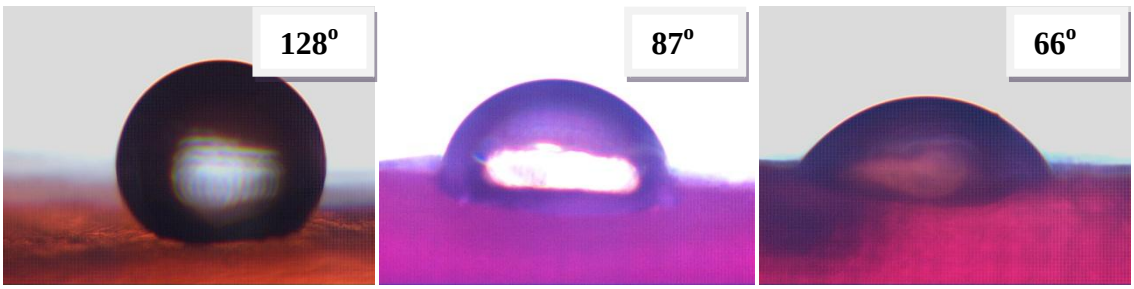

Figure 4.3 Image of water droplets on different hydrophobic aerogels

4.3 Effect of Hydrophobicity on Ketoprofen Release Behavior

The release experiments were carried out according to the procedure described in section 3.6 in a 0.1 N hydrochloric acid solution. The result of the release experiments demonstrated that immediate or sustained release of ketoprofen from non-coated aerogel was observed depending on the degree of hydrophobicity of aerogel As shown in figure 4.6, the drug release can be controlled by changing the hydrophobicity of the aerogel. As aerogels became more hydrophobic, the release rate gets slower. For hydrophilic aerogels, the release was completed nearly in 10 hours. However, for aerogels with contact angle 66^{o}, the release was completed in nearly 24 hours (Fig. 4. 6-a) . When the hydrophobicity of aerogel increased further, it was seen that release rate slowed further, too (Fig. 4. 6-b). Thus, alternation of hydrophobicity of the aerogel caused to decrease release rate because the penetration of water based release medium through the aerogel became difficult with increased hydrophobicity.

Beside these, it was observed that the hydrophilic aerogel lost its disk-shape during the release experiments and matrix erosion occurred. On the other hand, all hydrophobic aerogels preserved their original shapes during the experiment. The absence of matrix erosion was an indication that the release was governed mainly by diffusion, where zeroth-order release kinetics did not observed for hydrophobic aerogels. It should be also noted that ketoprofen loading capacity decreased down to 7 % (w/w) for the highest hydrophobicity conditions where the contact angle was measured as 128^{o}. 7 % by weight corresponds to nearly 5 mg for the typical disk shaped aerogels used in this study. However this amount can be increased up to 40 mg as the hydrophobicity of the aerogels was decreased.

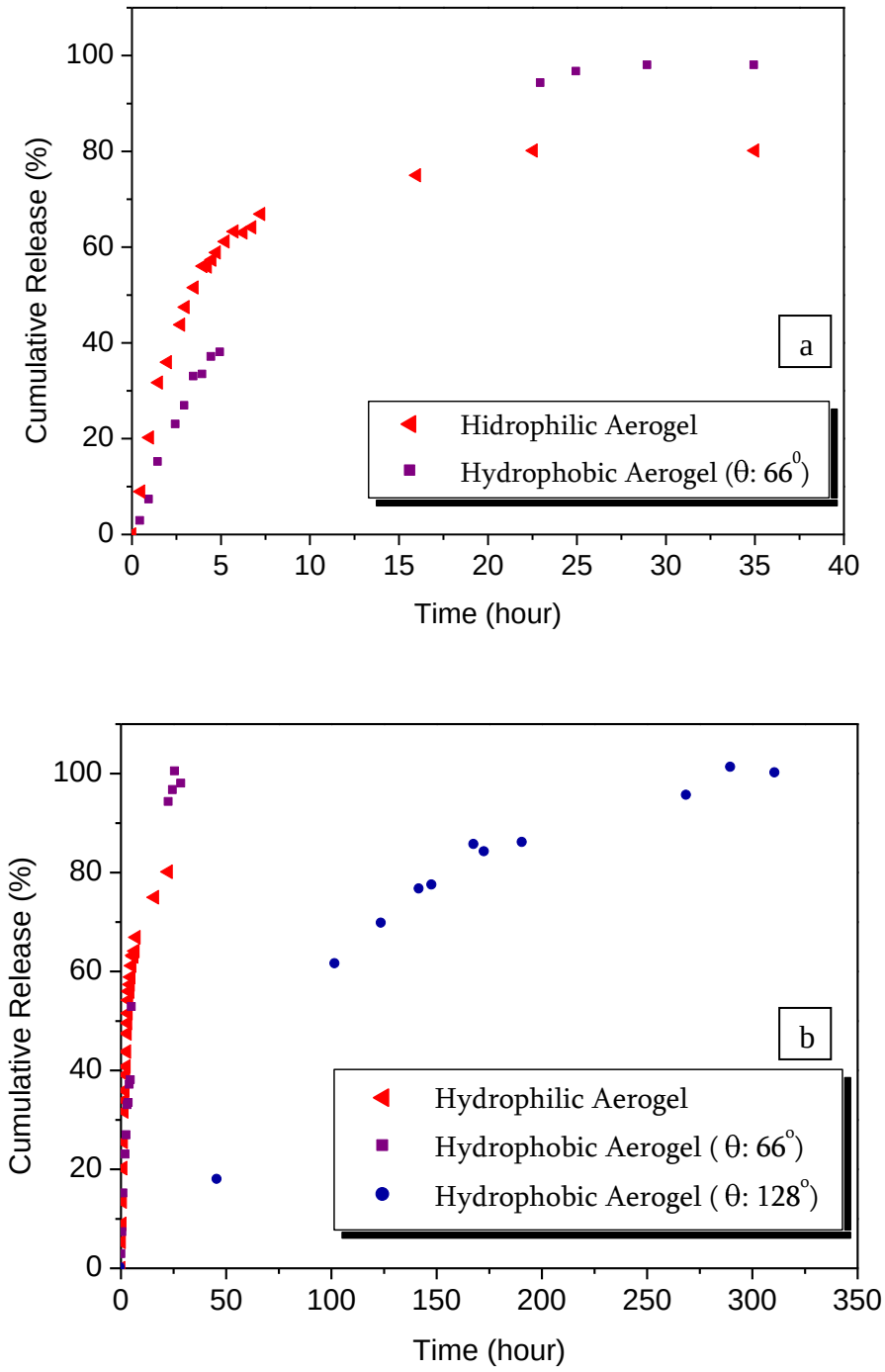

Figure 4.4 Release behavior of Ketoprofen from different hydrophobic aerogels in 100 ml of 0.1 N HCl solution at 37 °C and under constant string at 100 rpm

4.4 Ketoprofen Release from Coated and Non-Coated Hydrophilic Aerogels

In the previous section, effect of hydrophobicity of the aerogel on drug release was analyzed without using hydrogel coating. In this section, the release profiles from hydrogel coated aerogels were investigated.

It is known that the release rate of a drug from any medium depends on many different parameters such as the diffusion coefficient of the drug in the matrix, drug particle diameter, molecular weight of the drug, and drug solubility in the released medium, etc. In this study, hydrogel coating was used another way to control the release rate from aerogels. The effect of hydrogel coating was analyzed by alternation of concentration of the dimethacrylated PEG macromers which influence gel crosslinking density. Because the crosslink density affects the available free volume in the matrix for the movement of the drug molecules, the release rates from coated hydrogel differs as the PEG concentration of the hydrogel changes.

Figure 4.7 shows ketoprofen release rates from non-coated aerogel, and coated aerogels with hydrogels which have two different PEG concentrations; 15 % and 30 % by weight. As it is seen, the rate is the largest for non-coated hydrogel. As PEG concentration in the hydrogel coating increased, the release was hindered. As it is expected, the drug molecules cannot diffuse directly into the release media from the aerogel external surface due to the hydrogel coating. Thus, hydrogel coating was used as a barrier for the movement of the drug molecules. The porosity of hydrogel which depends on the crosslink density affects the diffusion coefficient of the drug in the hydrogel, and thus determines the release rate of drug.

In these experiments, all aerogels included nearly the same amount of drug which is around 40 mg. % 80 of cumulative release of that drug was reached for coated and non-coated samples which means drug did not accumulate between the mesh of hydrogel. In other words, if the drug molecule was big enough, it could be entrapped

into the hydrogel three dimensional networks. This could be explained by the low molecular weight (MW: 259 g) of the ketoprofen.

It must be pointed out that the hydrogel coating effect was examined by using hydrophilic aerogels not hydrophobic ones. Since the hydrogel coating for the most hydrophobic aerogel did not decrease the release rate further. However, the hydrogel coating effect can be used to retard the release rate for the hydrophobic aerogels with contact angle less then 128^{o}.

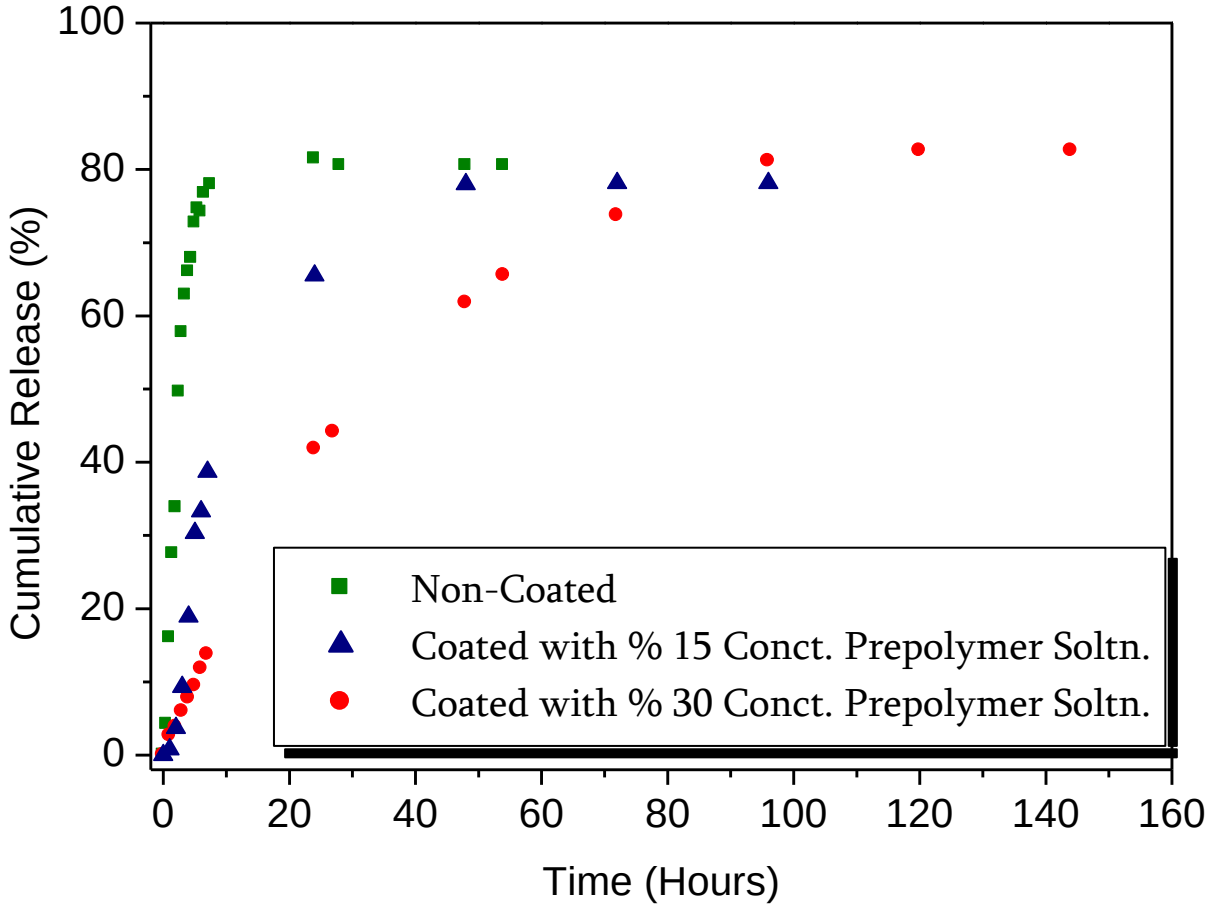

Figure 4.5 Release behavior of Ketoprofen from coated hydrophilic aerogels in 100 ml of 0.1 N HCl solution at 37 ^{o}C and under constant string at 100 rpm

Chapter 5

CONCLUSIONS

The novel composite of silica aerogel and PEG hydrogel was synthesized and its potential as a drug delivery system was investigated. Aerogels were synthesized by the two step sol-gel method using tetraethylortosilicate (TEOS) as the silica precursor. The alcogels were contacted with a solution of eosin-Y, a photoinitiator, dissolved in ethanol. After the drying procedure with $ScCO_2$, disk shaped Eosin-Y functionalized aerogels were produced. Then, silica aerogels were rendered hydrophobic using hexamethyldisilazane (HMDS) as the surface modification agent, and $ScCO_2$ (supercritical carbon dioxide) as solvent. Hydrophobicity of aerogel was tuned by changing HMDS amount dissolved in $ScCO_2$ phase which changes the contact angle between 0-128^o. For hydrogel coating, hydrophobic or hydrophilic aerogels were then dipped into a PEG diacrylate prepolymer solution, and photopolymerization was carried out using visible light (514 nm).

In the first part of this study, the novel composite was investigated. It is important to preserve the both aerogel and hydrogel structural properties during the synthesis. Thus, possible changes in the aerogel structure though synthesis processes were investigated by using nitrogen adsorption-desorption isotherms, BET surface area and BJH pore size calculations. As a result, two different structure such hydrophilic, wet network which is hydrogel and hydrophobic, dry network which is aerogel were successfully combined without losing their structural property. In the second part, the drug delivery application of this composite was studied. The effects of hydrophobicity of aerogel and PEG concentration of the hydrogel coating of hydrophilic aerogels on the drug release rate were examined. To test this ability, Ketoprofen was chosen as a model drug due to its well-known solubility in $ScCO_2$.

It was seen that, the drug loading capacity increases with decreased aerogel hydrophobicity while slower release rates are achieved with increased hydrophobicity from eosin functionalized aerogels. Indeed, it was seen that as the polymer concentration increased (0, 15 %, and 30 % by weight), the drug release was retarded. The experimental results show that the by using aerogel-hydrogel composite system, drug release can be controlled via changing hydrophobicity of the aerogel, and the concentration of the PEG in the hydrogel coating.

APPENDIX

1.1 Calibration Curve for Ketoprofen absorption at λ=260 nm

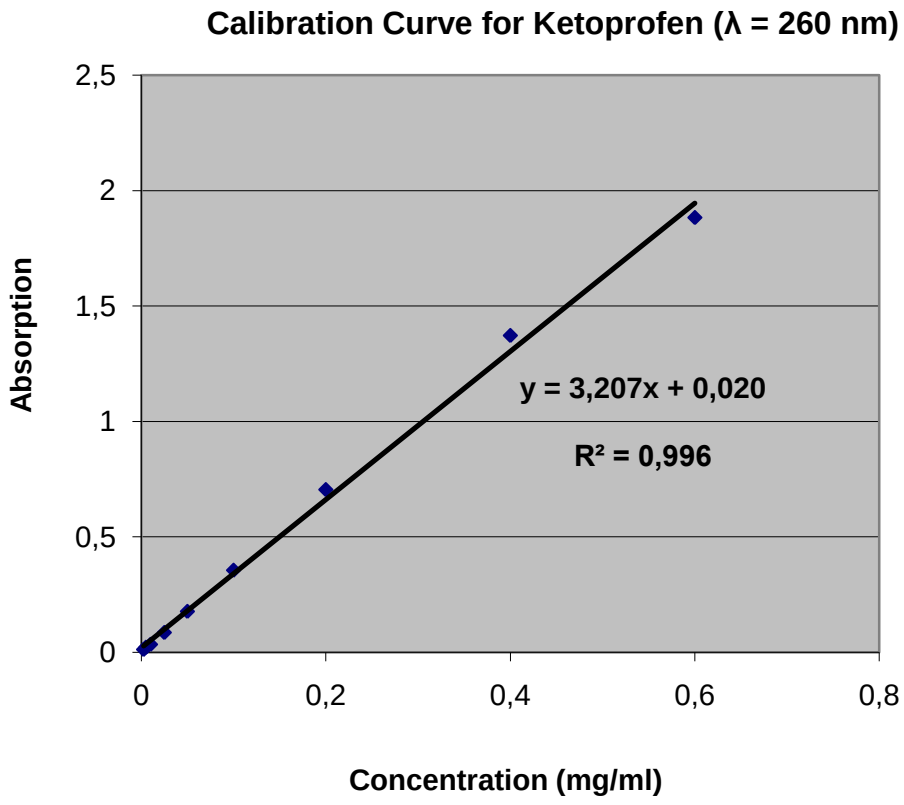

BIBLIOGRAPHY

[1] M. Stolarski, J. Walendziewski, M.S.B. Pniak, Synthesis and Characteristic of Silica Aerogels, Applied Cat. A. 177 (1999) 139-148.

[2] A.S. Dorcheh, M.H. Abbasi, Silica Aerogel;synthesis, properties and characterization, J. Materials Processing Tech. 199 (2008)10-26.

[3] L.W. Hrubesh, Aerogel Applications, J. Non-Cryst. Sol. 225 (1998) 335-342.

[4] M. Schmidt, F. Schwertfeger, Applications for silica aerogel products, J. Non-Cryst. Sol. 225 (1998) 364-368.

[5] J. Martin, B. Hosticka, C. Lattimer, P. M. Norris., Mechanical and acoustical properties as a function of PEG concentration in macroporous silica gels, J. Non-Cryst. Sol. 285 (2001) 222-229.

[6] A. Amlouk, L. El Mir, S. Kraiem, S. Alaya, Elaboration and characterization of TiO_2 nanoparticles incorporated in SiO_2 host matrix, J. Phys. Chem. Solids 67 (2006) 1464-1468.

[7] C. Erkey, Preparation of metallic supported nanoparticles and films using supercritical fluid deposition, J. Supercrit. Fluids 47 (2009) 517-522

[8] Smirnova, J. Mamic, W. Arlt, Adsorption of drugs on silica aerogels, Langmuir 19 (2003) 8521-8525.

[9] B.S.K Gorle, I. Smirnova, M.A. McHugh, Adsorption and thermal release of highly volatile compounds in silica aerogels, J. Supercrit. Fluids 48 (2009) 85-92.

[10] H Park, K. Park, Hydrogels in Bioapplications, in: R.M. Ottenbrite, S.J. Huang, K. PARK (Eds.) Hydrogels and Biodegradable Polymers for Bioapplications. ACS Symposium Series 627, American Chemical Society, Washington DC, 1996, pp. 2-11.

[11] N.A. Peppas, P. Bures, W. Leobandung, H. Ichikawa, Hydrogels in pharmaceutical formulations, European Journal of Pharmaceutics and Biopharmaceutics 50 (2000) 27-46.

[12] L. Bromberg, Crosslinked poly(ethylene glycol) networks as reservoirs for protein delivery, J. Appl. Polym. Sci. 59 (1996**)** 459-466.

[13] A.M. Lowman, N.A. Peppas, Analysis of the complex-ation/decomplexation phenomena in graft copolymer networks, Macromolecules 30 (1997) 4959-4965.

[14] S.Kızılel, V.H. Perez-Luna, F. Teymour, Mathematical Model for Surface-Initiated Photopolymerization of Poly(ethyleneglycol) Diacrylate, Macromol. Theory Simul. 15 (2006) 686-700.

[15] S. Kızılel, Photopolymerization of Poly(Ethylene Glycol) Diacrylate on Eosin-Functionalized Surfaces, Langmuir 20 (2004) 8652-8658.

[16] O. Valdes-Aguilera, C. P. Pathak, J. Shi, D. Watson, D. C. Neckers, Photopolymerization studies using visible light photoinitiators, Macromolecules 25 (1992) 541-547.

[17] S.S Kistler, Nature, 127 (1931) 741

[18] F. Schwertfeger, D. Frank, M. Schmidt , Hydrophobic waterglass based aerogels without solvent exchange or supercritical drying, J.Non-Cryst.Solids 225 (1989) 24-29.

[19] O. Masson, V. Rieux, R. Guinebretiere, A. Dauger, Size and shape characterization of TiO_2 aerogel nanocrystals, Nanostructured Materials, 7 (1996) 725-731.

[20] T. Horikawa, J. Hayashi, K. Muroyama, Size control and characterization of spherical carbon aerogel particles from resorcinol-formaldehyde resin, 42 (2004) 169-175.

[21] V. Stengl, S. Bakardjieva, M. Marikova, et al, Aerogel nanoscale aluminium oxides as a destructive sorbent for mustard gas, 47 (2003) 175-180.

[22] A.S. Dorcheh, M.H. Abbasi, Silica aerogel; synthesis, properties and characterizationjournal of materials processing technology, 199 (2008) 10–26.

[23] A.C. Pierre, G. M. Pajonk, Chemistry of aerogels and their applications, Chem. Rev. 102 (2002) 4243-4265

[24] B.R. Munson, D.F. Young, T.H. Okıishı, Fundementals of Fluid Mechanics, fifth edition, John Wiley & Sons, Inc. 2006

[25] S. G. Kazarian, Polymer Processing with Supercritical Fluids, Polymer Science, 42 (2000) 78–101

[26] F. Cansell , C. Aymonier, A. Loppinet-Serani, Review on materials science and supercritical fluids, Current Opinion in Solid State and Materials Science, 7 (2003) 331–340.

[27] F. Cansell, B. Chevalier, A. Demourgues, J. Etourneau, C. Even, V. Pessey, S. Petit, A. Tressaud, F. Weill, Supercritical fluid processing: a new route for materials synthesis J. Mater. Chem. 9 **(**1999) 67 – 75.

[28] C. Mantelis, T. Meyer, Supercritical Fluids, in Encyclopedia of Polymer Science and Technology. John Wiley & Sons, Inc.2008

[29] F. Cansell , C. Aymonier, A. Loppinet-Serani, Review on materials science and supercritical fluids, Current Opinion in Solid State and Materials Science, 7, (2003), 331–340.

[30] K.S.W. Sing, D.H. Everett, R.A.W. Haul, L. Mouscou, R.A. Pierotti, J. Rouquerol, T. Siemieniewska, Reporting physisorption data for gas/solid systems with special reference to the determination of surface area and porosity, Pure & Appl. Chem. 57 (1985) 603 - 619.

[31] L. Vrielink, BET: a practical approach, Group seminar Presentation, 13 June 2007 University of Twente.

[32] L. Lucarelli, Porosity and surface area by gas physisorption techniques, Thermo Electron Corporation presentation, 2003.

[33] M. Thommes, Nanoporous Materials –Science and Engineering, G.Q. Lu, X.S. Zhao, (Eds.) Chp. 11: Physical Adsorption Characterization of Ordered and Amorphous Mesoporous Materials, Imperial College Press,Vol. 4, 316-367.

[34] S. Brunauer, P.H. Emmett, E. Teller, Adsorption of gases in multimolecular layers**,** Journal of the American Chemical Society 60 (1938) 309-19.

[35] V. M. Gun'ko, M. S. Vedamuthu, G. L. Henderson, J. P. Blitz, Mechanism and kinetics of hexamethyldisilazane reaction with fumed silica surface, J. Colloid Interface Sci. 228 (2000) 157.

[36] A. V. Rao, G. M. Pajonk, S. D. Bhagat, P. Barboux, Comparative studies on surface chemical modification of silica aerogels based on various organosilane compounds of the type R_nX_{4-n}, J. Non-Cryst. Solids, 350 (2004) 216.

[37] A.M. Kartal, C. Erkey, Surface modification of silica aerogels by hexamethyldisilazane-carbon dioxide mixtures and their phase behavior, J. Supercrit. Fluids 53 (2010) 115-120.

[38] B. M. Novak, D. Auerbach, and C. Verrier, Low-Density Mutually Interpenetrating Organic-Inorganic Composite Materials via Supercritical Drying Techniques ,Chem. Mater., 6 (1994) 282.

[39] J. Premachandra et al, Preparation and Properties of Some Hybrid Aerogels from a Sulfopolybenzobisthiazole-Silica Composite. of Macromolecular Science, Part A, 36:1 (1999) 73 - 83.

[40] M.R. Ayersi A.J. Hunt, Synthesis and properties of chitosan- silica hybrid aerogels J. of Non-Crys, 285 (2001) 123-127.

[41] K. Kurumada et al. Nanoscopic replication of cross-linked hydrogel in high-porosity nanoporous silica , Journal of Non-Crystalline Solids, 353 (2007) 4839–4844.

[42] N. Leventis et al. Nanoengineered Silica-Polymer Composite Aerogels with No Need for Supercritical Fluid Drying, Journal of Sol-Gel Science and Technology, 35 (2005) 99-105.

[43] J. Martin, B. Hosticka, C. Lattimer and P. M. Norris, Mechanical and acoustical properties as a function of PEG concentration in macroporous silica gels, Journal of Non-Crystalline Solids, 285 (2001) 222-229.

[44] M.Prokopowicz, Silica-Polyethylene Glycol Matrix Synthesis by Sol-Gel Method and Evaluation for Diclofenac Diethyloammonium Release, Drug Delivery, 14:3 (2007) 129 - 138.

[45] M. Ahola, P. Kortesuo, I. Kangasniemi, J. Kiesvaara, A. Yli-Urpo, Silica xerogel carrier material for controlled release of toremifene citrate, International Journal of Pharmaceutics 195 (2000) 219-227.

[46] W. Dong, W. Lin, N. Contreras, D. Elmatari, Y. Lin, M. Torres, Pore Size Dependence of Proteinase K Diffusion Through Sol-Gel Dervied Silica, Mater. Res. Soc. Symp. Proc. 915 (2006) 9-17.

[47] D. Teoli, L. Parisi, N. Realdon, M. Guglielmi,A. Rosato, M. Morpurgo, Wet sol–gel derived silica for controlled release of proteins, Journal of Controlled Release 116 (2006) 295-303.

[48] E. M. Santos, S. Radin, P. Ducheyne, Sol-gel derived carrier for the controlled release of proteins, Biomaterials 20 (1999) 1695-1700.

[49] I. Smirnova, S. Suttiruengwong, W. Arlt, Feasibility study of hydrophilic and hydrophobic silica aerogels as drug delivery systems, Journal of Non-Crystalline Solids 350 (2004) 54–60.

[50] Irina Smirnova, S. Suttiruengwong, M. Seiler, W. Arlt, Dissolution Rate Enhancement by Adsorption of Poorly Soluble Drugs on Hydrophilic Silica Aerogels, Pharmaceutical Development and technology, 9 (2004) 443–452.

[51] C. C. Lin, and A. T. Metters. Hydrogels in controlled release formulations: Network design and mathematical modeling. Adv. Drug Deliv. Rev. 58 (2006) 1379–1408.

[52] C. Lin, K. S. Anseth, PEG Hydrogels for the Controlled Release of Biomolecules in Regenerative Medicine, Pharmaceutical Research, 26 (2009) 631-643.

[53] F. Quignard, R. Valentin, F. Di Renzo, Aerogel materials from marine polysaccharides, New J. Chem. 32 (2008) 1300–1310.

[54] M. Paakko, M. Ankerfors, H. Kosonen, A. Nykanen, S. Ahola, M. Osterberg, J. Ruokolaien, J. Laine, P. T. Larsson, O. Ikkala, et al. Enzymatic hydrolysis combined with mechanical shearing and high-pressure homogenixation for nanoscale cellulose fibers and strong gels, Biomacromolecules 8:6 (2007) 1934–1941

[55] M. Paakko, J. Vapaavouri, R. Silvenneoinen, H. Kosonen, M. Ankerfors, T. Lindstrom, L. A. Berglund, O. Ikkala, Long and entangled native cellulose I nanofibers allow flexible aerogels and hierarchically porous templates for functionalities, Soft Matter. 4:12 (2008) 2492–2499.

[56] L. M. Weber, C. G. Lopez, K. S. Anseth, Effects of PEG hydrogel crosslinking density on protein diffusion and encapsulated islet survival and function, Journal of Biomedical Materials Research Part A, 90A (2009) 720-729.

[57] G. M. Cruise, D. S. Scharp, J. A. Hubbell, Characterization of permeability and network structure of interfacially photopolymerized poly(ethylene glycol) diacrylate hydrogels, Biomaterials, 19 (1998) 1287-1294.

[58] F. Brandl, F. Kastner, R. M. Gschwind, T. Blunk, J. Teßmar, A. Göpferich, Hydrogel-based drug delivery systems: Comparison of drug diffusivity and release kinetics, Journal of Controlled Release 142 (2010) 221–228.

[59] D.C. Neckers, S. Hassoon, E. Klimtchuk, Photochemistry and photophysics of hydroxyfluorones and xanthenes. J. Photochem. Photobiol. 95 (1996) 33-39.

[60] J.S. Macnaughton, I. Kikic, Solubility of anti-inflammatory drugs in supercritical CO_2, J. Chem. Eng. Data 41 (1996) 1083-1086.